USGS
science for a changing world

A Computer-Aided Approach for Adapting Stage-Discharge Ratings and Characterizing Uncertainties of Streamflow Data with Discrete Measurements

Scientific Investigations Report 2022–5083

U.S. Department of the Interior
U.S. Geological Survey

Cover. The Pere Marquette River, Michigan. Photograph by Randall Schaetzl, Michigan State University.

A Computer-Aided Approach for Adapting Stage-Discharge Ratings and Characterizing Uncertainties of Streamflow Data with Discrete Measurements

By David J. Holtschlag

Scientific Investigations Report 2022–5083

U.S. Department of the Interior
U.S. Geological Survey

U.S. Geological Survey, Reston, Virginia: 2022

Suggested citation:
Holtschlag, D.J., 2022, A computer-aided approach for adapting stage-discharge ratings and characterizing uncertainties of streamflow data with discrete measurements: U.S. Geological Survey Scientific Investigations Report 2022–5083, 36 p., https://doi.org/10.3133/sir20225083.

ISSN 2328-0328 (online)

Acknowledgments

I would like to thank the authors of the freely available R packages mixed generalized additive model (GAM) computation vehicle (mgcv) and Multivariate Auto-Regressive State-Space (MARSS), which provided software tools needed for developing this report. I am also thankful to U.S. Geological Survey colleagues who collected streamflow data on Pere Marquette River that were used in this analysis. Finally, I would like to acknowledge the contributions of my U.S. Geological Survey colleagues who reviewed the manuscript and provided numerous improvements in the technical and editorial content of the report, the clarity of the illustrations, and the accessibility of the report through the internet.

Contents

Acknowledgments iii
Abstract 1
Introduction 1
Background 1
Purpose and Scope 2
Study Area 2
Discrete and Continuous Measurements at Streamgages 4
Discrete Measurements 4
Trends in Discrete Stage and Discharge Magnitudes 4
Time Between Discrete Measurements 4
Flow Control Conditions and Discharge Accuracy Qualifiers 6
Continuous Measurements 7
Frequencies of Unit Stage Data 7
Estimation of Missing Stage Data 9
Relation Between Discrete Stage Measurements and Daily Mean Stage 9
Frequency Density of Streamflow Data 9
Stage and Discharge Relations 9
Methods for Computer-Aided Adaptation of Stage-Discharge Ratings 12
Splines for Approximating Stage-discharge Ratings 14
Cubic Regression Spline Specification 14
Spline Parameters and Basis Values 15
Discrete-Time State-Space Model 15
State Equation 17
Initializing the State Vector 18
Measurement Equation 18
Measurement Time Series of Discrete Discharges 18
Design Array 19
Measurement Error Variance 19
Methods for Computing Magnitudes and Uncertainties of Unit Discharges 19
Kalman Filtering 19
Kalman Smoothing 20
Results and Discussion 21
Cubic Regression Splines 21
State-Space Modeling 22
Development of State-Space Models 24
Changes in Hyperparameters of Cubic Regression Spline 24
Stage-discharge Rating Adaptations with Discrete Measurements 26
Discharge Magnitudes and Uncertainties of the Kalman Smoothed Discharges 26
Comparison of Rated and Smoothed Discharges with Published Daily Means 26
Limitations 34
Summary and Conclusions 34
References Cited 35

Figures

1. Map showing the study area near U.S. Geological Survey streamgage 04122500 Pere Marquette River at Scottville, Michigan 3
2. Graphs showing discrete flow measurements at 04122500 Pere Marquette River at Scottville, Michigan, from 1985 to 2020 5
3. Graph showing time between discrete measurements at Pere Marquette River from 1985 to 2020....6
4. Graph showing the number of unit stage values per day from water years 1990 to 2020 obtained at U.S. Geological Survey streamgage 04122500 Pere Marquette River at Scottville, Michigan....8
5. Graph showing measured and estimated daily mean stage at U.S. Geological Survey streamgage 04122500 Pere Marquette River at Scottville, Michigan 10
6. Graph showing relation between discrete stage and daily mean stage at U.S. Geological Survey streamgage 04122500 Pere Marquette River at Scottville, Michigan....11
7. Graph showing probability density of daily mean flows at U.S. Geological Survey streamgage 04122500 Pere Marquette River at Scottville, Michigan, from water years 1990 to 2019 12
8. Graph showing discrete measurements with base rating curves for U.S. Geological Survey streamgage 04122500 Pere Marquette River at Scottville, Michigan....13
9. Graphs showing basis values for cubic regression splines computed from rating curve tables at U.S. Geological Survey streamgage 04122500 Pere Marquette River at Scottville, Michigan....16
10. Graphs showing rated discharge curve with cubic regression spline estimates of the magnitude and uncertainty of the rating based on discrete discharge measurements for U.S. Geological Survey streamgage 04122500 Pere Marquette River at Scottville, Michigan....23
11. Graphs showing hyperparameters of cubic regression spline developed in state-space model 6 for U.S. Geological Survey streamgage 04122500 Pere Marquette River at Scottville, Michigan....25
12. Graphs showing adapted rating computed using Kalman smoothing parameters with discrete measurements from 1990 to 2018 for U.S. Geological Survey streamgage 04122500 Pere Marquette River at Scottville, Michigan....27
13. Graphs showing measures of daily mean discharge magnitudes and uncertainties for selected water years at U.S. Geological Survey streamgage 04122500 Pere Marquette River at Scottville, Michigan 28
14. Graph showing relation between discharges computed with rating 18 and published daily mean discharges for water years 1990 through 2019 at U.S. Geological Survey streamgage 04122500 Pere Marquette River at Scottville, Michigan....29
15. Graph showing relation between discharges computed with base ratings 18–21 and published daily mean discharges for water years 1990 through 2019 for U.S. Geological Survey streamgage 04122500 Pere Marquette River at Scottville, Michigan....30

16. Graph showing relation between Kalman smoothed discharge estimates and published computed daily mean discharges for water years 1990 through 2019 for U.S. Geological Survey streamgage 04122500 Pere Marquette River at Scottville, Michigan....32
17. Graph showing distribution of differences between smoothed and computed daily mean discharges for water years 1990 through 2019 at U.S. Geological Survey streamgage 04122500 Pere Marquette River at Scottville, Michigan....33

Tables

1. Channel conditions and flow accuracy qualifiers during selected discrete flow measurements at USGS streamgage 04122500 Pere Marquette River at Scottville, Michigan, from 1985 through 2019....7
2. Selected rating periods for U.S. Geological Survey streamgage 04122500 Pere Marquette River at Scottville, Michigan....9
3. Summary statistics for five-knot cubic regression splines for rating periods 18–21 at U.S. Geological Survey streamgage 04122500 Pere Marquette River at Scottville, Michigan....21
4. Initial state vector estimate based on spline parameters for expanded stage-discharge rating 18 at U.S. Geological Survey streamgage 04122500 Pere Marquette River at Scottville, Michigan....22
5. Alternative state-space models developed for adaptive ratings at U.S. Geological Survey streamgage 04122500 Pere Marquette River at Scottville, Michigan....24

Conversion Factors

U.S. customary units to International System of Units

Multiply	By	To obtain
	Length	
foot (ft)	0.3048	meter (m)
mile (mi)	1.609	kilometer (km)
	Area	
acre	0.4047	hectare (ha)
square mile (mi^2)	2.590	square kilometer (km^2)
	Volume	
ounce, fluid (fl. oz)	29.57	milliliter (mL)
	Flow rate	
foot per second (ft/s)	0.3048	meter per second (m/s)
cubic foot per second (ft^3/s)	0.02832	cubic meter per second (m^3/s)

Datums

Vertical coordinate information is referenced to the North American Vertical Datum of 1988 (NAVD 88).

Elevation, as used in this report, refers to distance above the vertical datum.

Stage, as used in this report, refers to distance above gage datum.

Supplemental Information

A water year is the period from October 1 to September 30 and is designated by the year in which it ends; for example, water year 2015 was from October 1, 2014, to September 30, 2015.

Note: In this report, the notation is generally consistent with notation used in the Multivariate Auto-Regressive State-Space (MARSS) package (Holmes and others, 2020b). Some adaptations were applied to conform to conventions that are specific to the application. In particular, scalars are indicated by italic lowercase Latin or Greek characters; scalar time series are also lower case but are subscripted with a time index. Vectors are indicated by bold italic lowercase characters, and vector time series are subscripted with the time index. In general, states and measurements can be scalar or vector time series. In this report, however, the states are vector series shown as x_k, whereas the measurements are scalar series shown as y_k. Matrices are indicated by italic uppercase characters. Matrices subscripted with a time index are time varying matrices but are referred to as an array in R.

Abbreviations

AIC	Akaike information criterion
CRS	cubic regression spline
GAM	generalized additive model
MARSS	Multivariate Auto-Regressive State Space, an R package
mgcv	mixed GAM computation vehicle, an R package
NWIS	National Water Information System
USGS	U.S. Geological Survey

A Computer-Aided Approach for Adapting Stage-Discharge Ratings and Characterizing Uncertainties of Streamflow Data with Discrete Measurements

By David J. Holtschlag

Abstract

Relations between stage (water level) and discharge of streamflow through a natural channel are the result of time-varying processes, which are commonly described by time-varying stage-discharge ratings. Hydrographers with the U.S. Geological Survey successfully maintain the accuracy of streamflow data by manually applying time-tested approaches to adapt ratings to temporal changes in hydraulic conditions. The difficulty with the manual approach is that it is a subjective, time-consuming process that requires considerable skill and experience to implement. In addition, manual adjustments of ratings make quantification of resulting streamflow data uncertainties problematic. A computer-aided adaptive stage-discharge estimation approach is proposed to track sequential changes in the relation between stage and discharge at continuous-record streamgages. In this report, adaptations are based strictly on discrete measurement data that are then used to compute the magnitudes and uncertainties of streamflow. The approach entails the parameterization of a cubic regression spline (CRS) for the stage-discharge relation based on an existing rating or on a set of discrete measurements. A state-space model is then parameterized to track temporal changes in stage-discharge relations beginning with the initial CRS parameterization using discrete measurements. Finally, Kalman estimation is used with the state-space model to estimate the magnitude and uncertainty of flows. In a case study using data from streamgage U.S. Geological Survey 04122500 Marquette River at Scottville, Michigan, a five-parameter CRS model was estimated from data in an existing stage-discharge rating to provide an initial CRS parameter set for a state-space model. The initial CRS parameters were updated sequentially in a state-space model based on periodic discrete measurements of stage and discharge that spanned a 30-year period for this analysis. Additional analysis is needed to determine the timing of rapidly varying shifts more precisely in stage-discharge relations than the relatively infrequent discrete measurements currently enabled. Unit streamflow estimates based on flow in a local streamgaging network may provide a basis for adapting a stage-discharge rating at unit time intervals by augmenting discrete measurement data within the state-space model.

Introduction

Introductory material contains background information on streamgaging, the purpose and scope of the study, and site characteristics for the case study.

Background

The U.S. Geological Survey (USGS) currently (2021) publishes streamflow data at approximately 8,500 active streamgages throughout the United States. Streamgages measure outflow from a basin, which is topographically defined by the drainage divide. Stage data are used to compute unit values of flow based on a monotonically increasing relation between stage and discharge. A rating is developed and maintained based on discrete, contemporaneous measurements of stage and discharge that span the range of flows of interest at the streamgage. Discrete stage and streamflow measurements require field visits to streamgages, which is a substantial component of the costs of streamgage operations.

The stage-discharge relation described by a rating can change gradually with time because of persistent changes in the geometry or hydraulic conditions across a riffle (section), channel, or overbank control. Alternatively, the relation can change abruptly owing to intermittent effects such as increased backwater associated with seasonal aquatic plant growth or ice formation. Once the cause of the intermittent changes is no longer in effect, the stage-discharge relation may revert to nominal conditions consistent with possible persistent changes in the stage-discharge relation. Commonly, persistent and intermittent changes affect stage-discharge relations. The distinction between persistent and intermittent changes is somewhat arbitrary but practically determined by the frequency of discrete measurements. Intermittent changes,

such as ice backwater effects, have time scales of hours to days during periods when no discrete measurements are taken to identify the onset, cessation, or variable magnitude of backwater associated with these intermittent changes.

The USGS publishes daily mean flows that are qualified as either computed or estimated. Computed daily mean flows are based on the average of daily unit flows. Unit flows are computed by use of the stage-discharge rating and continuous unit stage data. Computed flows are commonly determined from an expanded rating table (0.01-foot [ft] increments of stage) using a base rating or a version of the base rating that has been adjusted or shifted to better reflect hydraulic conditions at the time of stage measurement. These rating shifts are needed and greatly enhance the accuracy of the computed flow record. The traditional analysis of shifts, however, is a subjective and time-consuming process that makes quantifying the uncertainty of the flow record problematic. At certain points in time, the shifts so predominate the computation of flows that a new base rating is developed to account for persistent hydraulic changes that were previously characterized by a series of temporary shifts. Subsequent shifts are then applied to the revised base rating. When stage data are missing, or perhaps inapplicable because of variable backwater conditions, flows are qualified as estimated, which may be based on a relation between flows at the target streamgage and flows at other streamgages in the network.

In this report, an alternative approach for computing flows is developed and evaluated that also requires continuous stage data and discrete measurements. To facilitate comparisons of the conventional and alternative approaches, some simplifications to standard computational conventions (Rantz, 1982a) are used that reduce the computational effort without invalidating the comparisons; for example, daily mean flows were computed by use of daily means of unit stages, rather than daily means of unit flows computed from unit stages. These differences, however, tend to decrease with decreasing variability of unit flows, which is more common at moderate to large streams than for small streams.

Base ratings are seldom used for extended periods without shifts to compute published streamflow data; furthermore, the accuracy of the base rating, if it were applied without shifts throughout the period when the base rating was nominally in effect, would not accurately reproduce streamflow characteristics. Instead, the difference between the accuracy of the base rating and the accuracy of the streamflow record indicates the value of shifts and other adjustments applied to improve the accuracy of the streamflow record. The fundamental question addressed in this report is whether these shifts can be computed from discrete flow measurement data to adapt the rating in a way that would require less subjective intervention and make it feasible to statistically characterize the uncertainty of the streamflow record more accurately than the current approach.

Purpose and Scope

The purpose of this report is to describe the initial development of a computer-aided approach for adapting stage-discharge ratings to changes in hydraulics at streamgages based on discrete measurements of stage and discharge. In addition to rating adaptation, the approach provides a basis for estimating the magnitudes and uncertainties of streamflow data. The low frequency of discrete measurements relative to the higher frequency of some intermittent changes in hydraulic conditions, however, limits the temporal resolution for adapting a rating to times of discrete measurements.

Data from USGS streamgage 04122500 Marquette River at Scottville, Michigan (U.S. Geological Survey, 2022), for the 30-year period of analysis from October 1, 1989, to September 30, 2019 (water years 1990 to 2019), were used as a case study. This period was considered sufficiently long to demonstrate the utility of the approach by estimating substantial changes in stage-discharge relations documented at the streamgage during an extended period. Given the extended period of analysis and the restrictions associated with discrete measurements, however, a 1-day time step was used to illustrate the approach. During this period of analysis, computed (rather than estimated) daily mean flows were used for model comparison. Most of the estimated daily mean flows were ice-affected and thus not used in model comparison. Although the proposed model structure is thought to be adaptable to the computation of ice-affected streamflow and network flows could be used to refine the resolution of shifts, this capability is not developed in this initial implementation.

Study Area

Data from the 04122500 Pere Marquette River at Scottville, Mich. (Pere Marquette streamgage) were used in this analysis. The Pere Marquette River at the streamgage drains a basin of 681 square miles in the west central lower peninsula of Michigan (fig. 1). The basin is generally forested and includes parts of the Huron-Manistee National Forest. Flow has been measured continuously at the streamgage starting in August 1939 and was active at the time this report was prepared (March 2022).

The Pere Marquette streamgage was selected because it has an extended period of data to support the analysis, and streamflow records indicate a pronounced and consistent tendency for channel degradation. Electronically accessible records include unit (shorter than daily interval) stage data beginning in October 1989 to present. Daily mean streamflow data are available from April 1939 to present. Discrete (paired stage and discharge) measurement data obtained during field visits are available electronically beginning in August 1985 (https://waterdata.usgs.gov/nwis/measurements/?site_no=04122500, accessed June 17, 2022). In addition, expanded (0.01-ft interval) stage-discharge rating tables, used as a basis to compute unit flow values, are electronically accessible

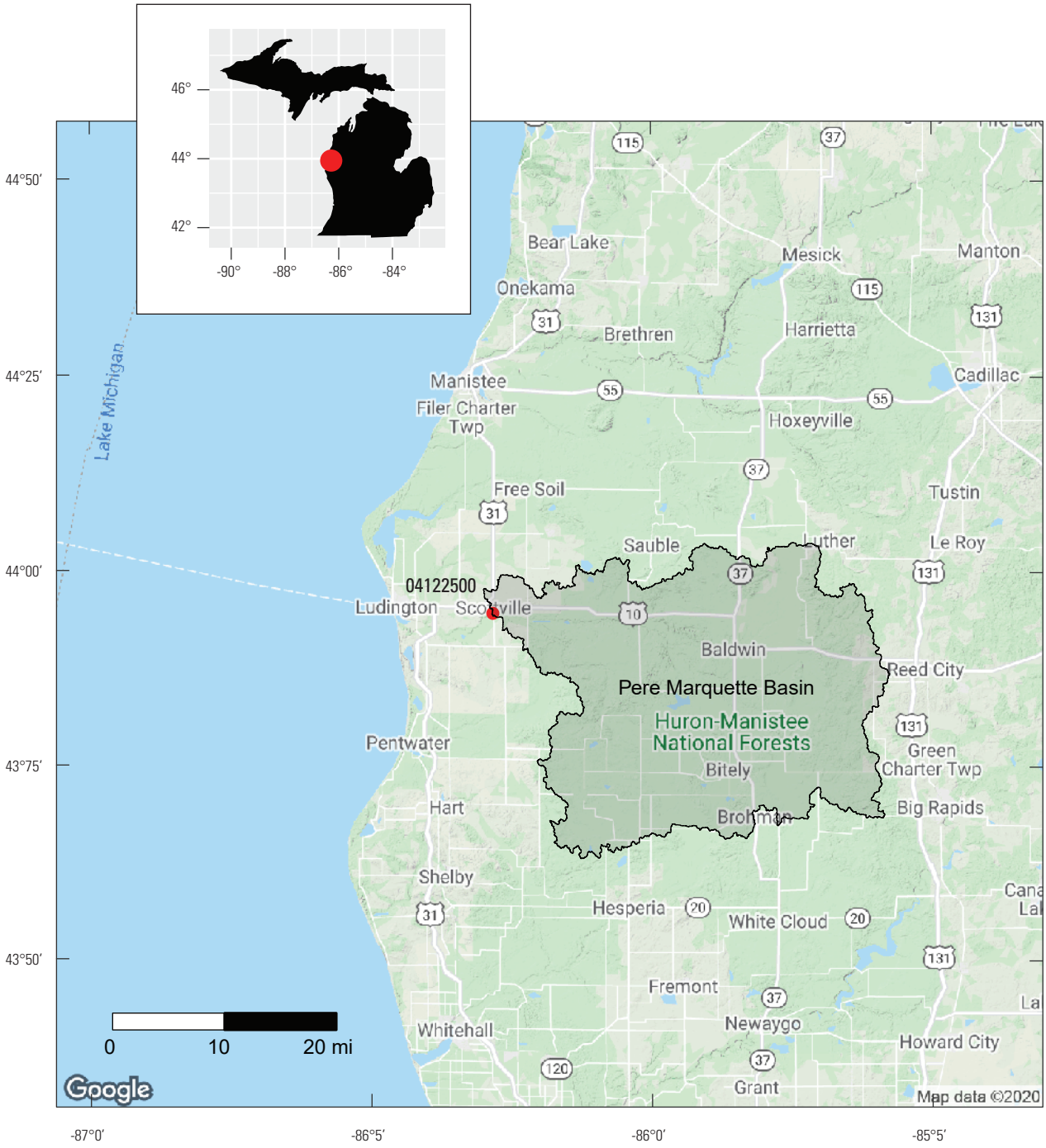

Figure 1. The study area near U.S. Geological Survey streamgage 04122500 Pere Marquette River at Scottville, Michigan.

(https://waterdata.usgs.gov/nwis/uv?site_no=04122500, accessed June 17, 2022). For this study, ratings 18, 19, 20, and 21 were used corresponding to the period from October 1986 to October 2019. These ratings indicate a persistent and conspicuous change that generally enables a lower stage to pass the same flow as earlier stage-discharge relations; for example, rating 21 passes 55.1 percent more flow than rating 18 at 1.4 ft of stage. This increase diminishes to 12.3 percent more flow at 8.0 ft of stage.

Persistent changes in stage-discharge relations at the Pere Marquette streamgage may be related to streambed stability as the sand channel has shown appreciable local scour near the streamgage on South Scottville Road bridge over the Pere Marquette River during high-flow events; for example, on September 13, 1986, discrete flow measurement number 479 of 6,440 cubic feet per second (ft^3/s) was obtained at the streamgage, with a maximum local streambed scour of 1.55 ft relative to the streambed indicated by previous measurements. Four days later, discrete flow measurement number 480 of 2,610 ft^3/s was obtained in which a maximum local streambed scour of 4.06 ft was measured (Holtschlag and Miller, 1998). Subsequent discrete measurements indicated that the scour hole had refilled. The utility of the proposed approach for tracking changes in the stage-discharge relation, however, is not thought to require a conspicuous trend. In addition to the persistent trend, intermittent seasonal ice effects periodically increase the stage needed to pass a given flow than during open-water conditions.

Discrete and Continuous Measurements at Streamgages

This section discusses types of discrete and continuous measurements made at streamgages and how this information is used together for streamflow computation. Contemporaneous discrete measurements of stage and discharge are used to define and update the generally time-varying relation between stage and discharge. An initial set of measurements is typically constrained in time but span the range of stages and flows that are typical at the streamgage. This initial set of measurements is used to develop the initial stage-discharge rating. Continuous measurements of stage are then used with the stage-discharge relation to compute continuous records of streamflow.

Discrete Measurements

Discrete measurements refer to paired field measurements of stage and discharge commonly made at 6- to 8-week intervals. Discrete measurements are used to develop, confirm, or update the stage-discharge rating. A base rating is initially developed from a set of discrete measurements at a new or reactivated streamgage. Consistency of subsequent discrete measurements with the existing rating confirm the rating; inconsistencies may indicate the need to adapt the existing rating by use of a shift.

The localized discrepancy between an existing rating and a discrete measurement indicates the approximate magnitude of a shift although the applied shift may be reduced because of the uncertainty of the streamflow measurement. The measured stage value may indicate which control feature (a riffle, channel, or overbank area) may have changed. The timing of discrete measurements, however, only approximates the timing of the changes in hydraulic controls. This approximation becomes coarser with increasing time intervals between discrete measurements. A control can change suddenly as the result of high flow event, or the control can change gradually because of vegetation growth in the channel. Hydrographers may use streamflow information in the local streamgage network to refine estimates of the timing of changes in the control.

With time, an accumulation of overlapping shifts may obscure the changes to the base rating. When changes are obscured, the base rating is revised, and the rating number is incremented to reference the changed conditions. Subsequent shifts are then referenced to the revised base rating.

Once a rating is defined, it can be used with continuous stage data and information on the timing and magnitude of shifts to compute corresponding continuous streamflow data. The data represent the average flow during regularly spaced short intervals of time, which is referred to as "unit" data. Unit data typically vary in length from 5 to 60 minutes. Historically, streamflow data have been aggregated from unit to daily mean values.

Trends in Discrete Stage and Discharge Magnitudes

Figure 2 shows a time series plot of discrete discharge and stage measurements from 1986 to 2020. There is no statistically significant trend in the magnitudes of discharge (discharge panel: p=0.9336). There is, however, a statistically significant negative trend in stage (stage panel: p=7.532×10^{-05}) during the same period. Given the lack of trend in discharge values, the decreasing trend in stage values may be interpreted as increasing channel conveyance at lower stages rather than diminishing flows. These changes in conveyance may be reflected in a systematic change in the stage-discharge relations with time. The variability of stage values may be increasing during analysis (fig. 2).

Time Between Discrete Measurements

The frequency of discrete measurements determines the frequency of adaptations to the stage-discharge relation in the proposed approach. Figure 3 shows the irregular time series of discrete measurements and a histogram of time between measurements on the right. Time between discrete

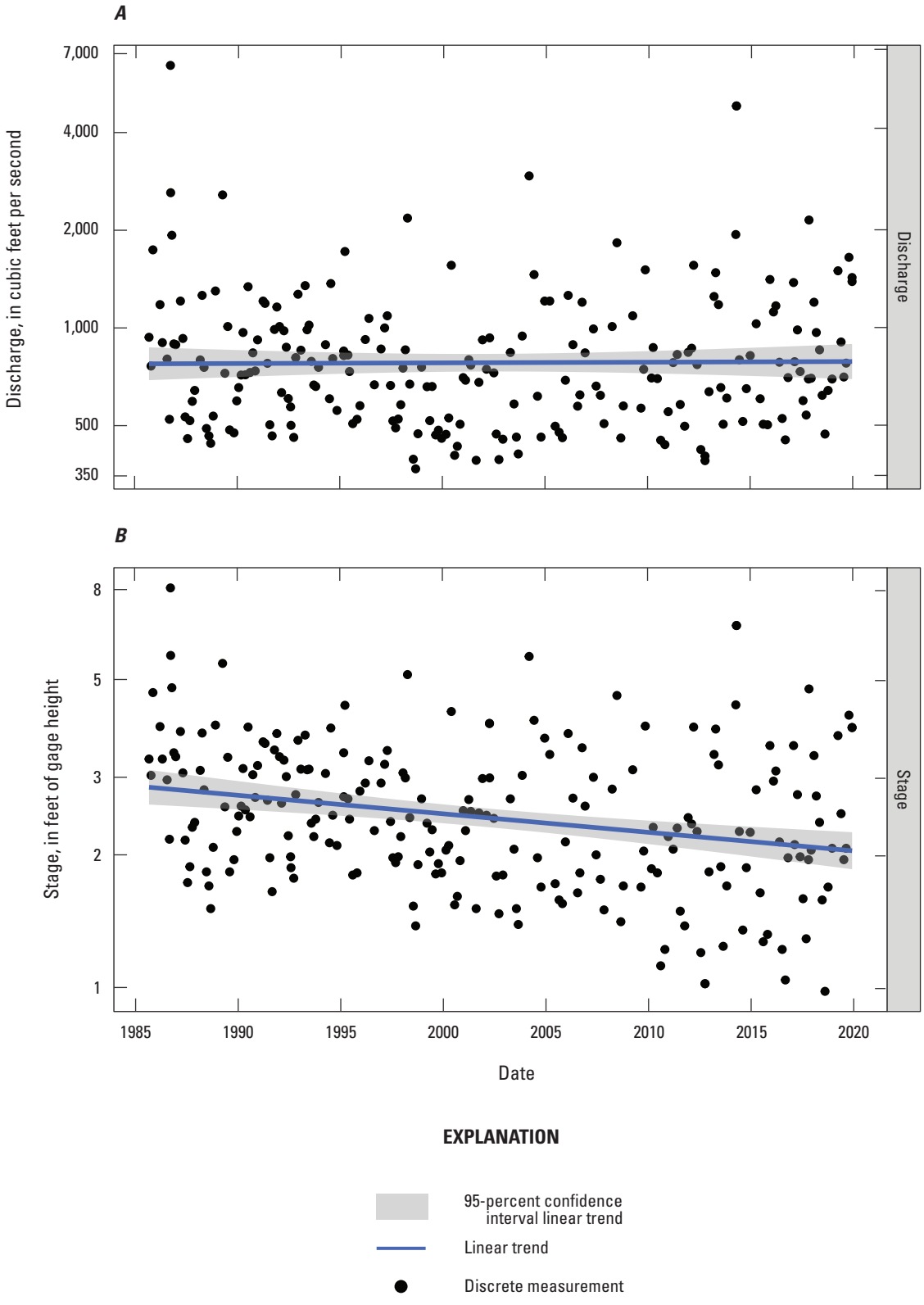

Figure 2. Discrete flow measurements at 04122500 Pere Marquette River at Scottville, Michigan, from 1985 to 2020.

measurements was computed to the nearest day. Based on the selected discrete measurements at Pere Marquette River, the mode of the distribution of time between discrete measurements was 42 days and the mean was 56.9 days. There is some evidence from the plot that the time between discrete measurements increased (measurement frequency decreased) after 1993. There are no extended gaps in discrete flow measurements. Occasionally check measurements are made immediately after an initial flow measurement to confirm its accuracy. A check measurement is a second measurement on the same day and flow conditions to confirm the accuracy of the initially measured flow. An average flow was computed from the two measurements on the same day to represent the discrete flow measurement for that day.

Flow Control Conditions and Discharge Accuracy Qualifiers

Discrete measurement data for the Pere Marquette streamgage were retrieved from the USGS National Water Information System (NWIS) using the dataRetrieval package (De Cicco and others, 2018) in R (R Core Team, 2021). Table 1 summarizes the type of flow control, characterized with the table heading "Control conditions" and the accuracy of discrete flow measurements indicated by the table heading "Flow accuracy qualifier." Control conditions and flow accuracy qualifiers are assigned by hydrographers in the field based on flow measurement criteria provided by Rantz (1982a). Control conditions are categorized in this report as: "Clear channel," "Light vegetation," "Light debris," "Shore ice," "Moderate debris," and "Ice cover." The most common control condition was "Clear channel," and the most common flow measurement accuracy qualifier was Good.

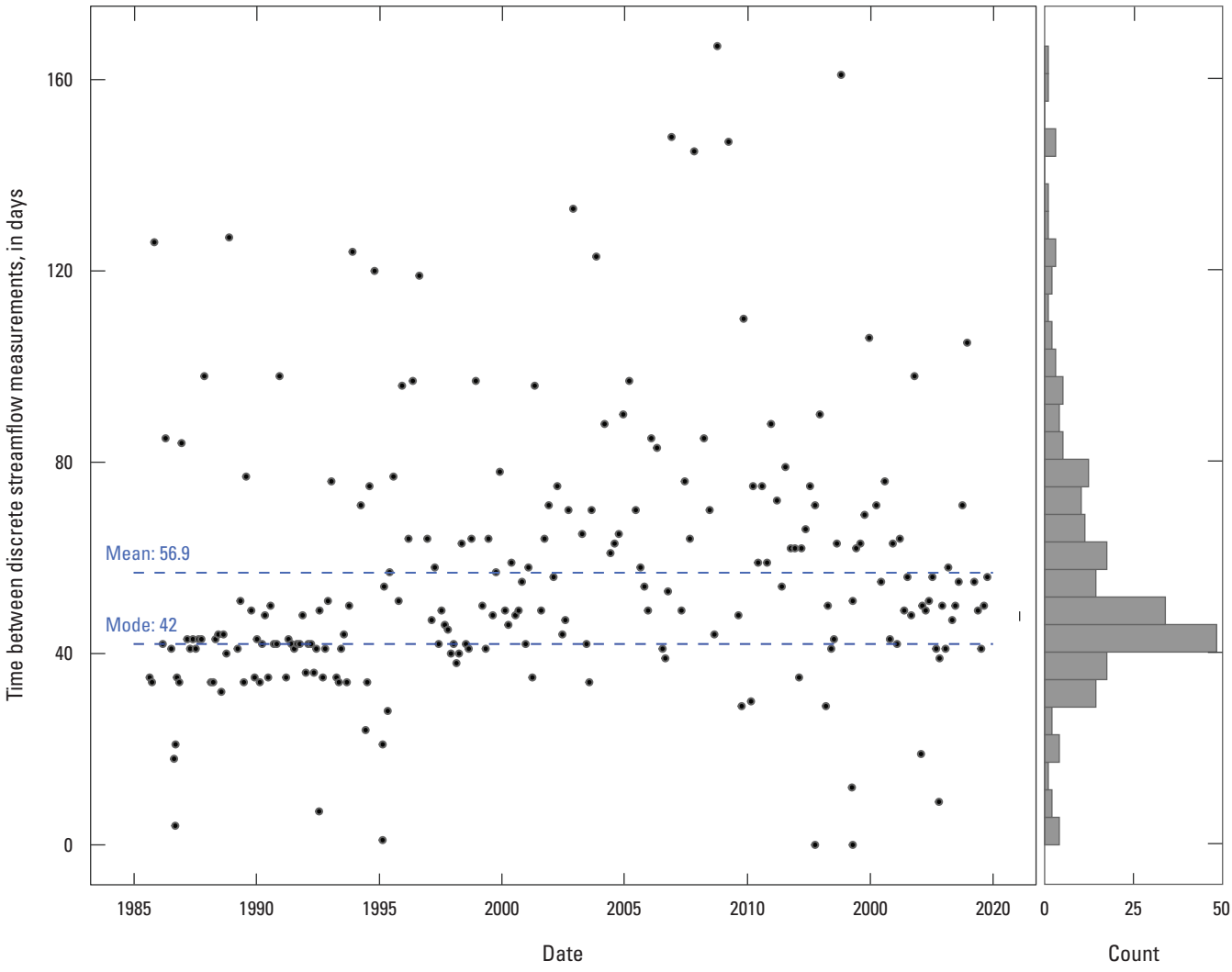

Figure 3. Time between discrete measurements at Pere Marquette River from 1985 to 2020.

Table 1. Channel conditions and flow accuracy qualifiers during selected discrete flow measurements at USGS streamgage 04122500 Pere Marquette River at Scottville, Michigan, from 1985 through 2019.

[NA, not applicable]

Control conditions	Flow accuracy qualifier (nominal error				
	Excellent (2 percent)	Good (5 percent)	Fair (8 percent)	Poor (12 percent)	Total
Clear channel	0	184	10	0	194
Light vegetation	0	1	0	0	1
Light debris	0	11	0	0	11
Shore ice	0	5	5	1	11
Moderate debris	0	5	0	0	5
Ice cover	0	4	1	2	7
Total	0	210	16	3	229

Ice-affected measurements were removed from the analysis because during periods of ice effect, published flows are often estimated rather than computed. These included all measurements of control type “Ice covered” and measurements numbered 474 and 657 obtained on January 28, 1986, and December 11, 2013, respectively. The measurements indicated the control conditions as “Shore Ice,” but had departures from open-water ratings that were more consistent with “Ice covered” measurements. These two measurements were qualified as Fair and Poor, respectively (table 1).

The flow accuracy qualifiers assigned to discrete measurements were used to estimate measurement error variances (uncertainties) of the measured flows. In this paper, a qualifier of Excellent indicates that measured flows are within 2 percent of the actual flows; Good indicates that measured flows are within 5 percent; Fair indicates that measured flows are within 8 percent; and Poor indicates that measured flows are within 12 percent of actual flows. The associations are based on the “Discharge Measurement Quality Code” descriptions by U.S. Geological Survey (2011). These low percentage errors correspond closely to errors in natural logarithm units.

Continuous Measurements

Continuous measurements of stage are typically acquired by automated recorders of water-levels from float sensors, pressure transducers, or other means (Rantz, 1982a). Stage is commonly referenced to a gage datum and to a standard vertical datum. It may be convenient to think of a 0.0-ft gage height as the minimum elevation in the channel where the stream is being monitored or the point of zero flow. A gage height of 1.0 ft would then correspond to a maximum depth of water of 1.0 ft in the stream. To avoid recording negative stages should a channel erode, the initial point of zero flow is commonly placed below the minimum depth in the channel. Stages can be converted to a water-surface elevation by adding the standard vertical datum to the gage height.

The Pere Marquette streamgage has a standard vertical datum of 597.47 ft above the North American Vertical Datum of 1988 (NAVD 88). Thus, a gage height of 1 ft would indicate a water-surface elevation that is 598.47 ft above NAVD 88. Stage values referenced to a gage datum are more sensitive to scale transformations than stage values referenced to a standard datum. In this report, square root transformations are applied to gage heights rather than water-surface elevations to help linearize the relation between stage and the logarithm of flow.

Stage measurements are frequently transmitted to USGS processing centers to provide near real-time stage and discharge data. Stage measurements are used to compute a preliminary flow value based on the current rating. The preliminary values of stage and discharge may be updated after subsequent discrete measurements have been obtained and quality assurance techniques have been applied.

Historically, unit and daily stage data were considered to be auxiliary measurements in the computation of flows; thus, there is less electronic accessibility of unit and daily stage data than daily mean flow data. Limitations in the availability of historical stage data constrained the start of the period of analysis used in this report, although the amount of available stage data is sufficient to support the analysis.

Frequencies of Unit Stage Data

There is no standard for the frequency of unit value collection. These frequencies may vary with the size of the basin, topographic and soil characteristics, vegetative cover, flow regulation, and other factors to capture the streamflow variability. At the Pere Marquette streamgage, the number of unit values recorded per day varied during the period of the analysis (fig. 4). Frequencies from October 1, 1989, to May 4, 1994, generally averaged 24 values per

day (hourly data); from May 5, 1994, to February 21, 1997, 288 values per day (5-minute interval data) were common; and after February 21, 1997, 96 values per day (15-minute interval data) were common, as indicated by the apparently solid black lines. Small irregularities (individual dots) associated with missing unit values are present during analysis at all regular measurement frequencies.

In developing the computer-aided adaptive approach, a simple method was used to adjust for changing frequencies or the absence of unit (or daily) stage data. For periods when unit stage data was available, a daily mean value was computed from all unit stage data for that day. On days when no unit (or daily) stage data were available, the published daily mean flow was used with an inverse application of the stage-discharge rating to estimate a daily mean stage. This allowed model computations to proceed simply at daily time steps rather than variable unit time steps. In addition, unit time steps would have substantially increased the computational requirements for parameter estimation in the state-space model with little benefit.

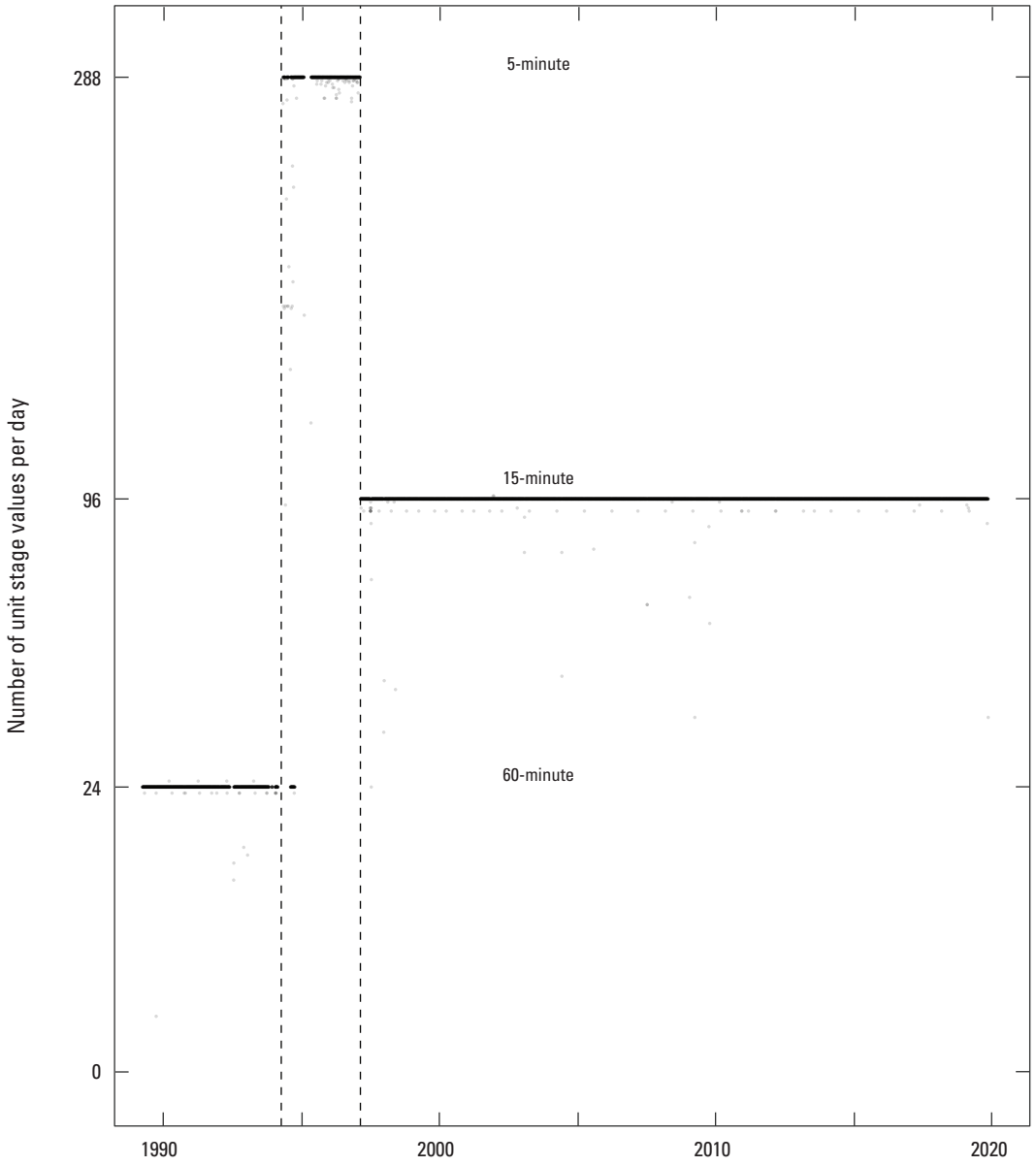

Figure 4. Number of unit stage values per day from water years 1990 to 2020 obtained at U.S. Geological Survey streamgage 04122500 Pere Marquette River at Scottville, Michigan.

Estimation of Missing Stage Data

The time series of computed daily mean stage values (fig. 5) shows a seasonal variation within which annual minimums appear to have a downward trend. During the early 1990s, minimum annual stage values were generally greater than 1.6 ft above gage datum, while during the 2010s, minimum annual stage values were generally 0.6 ft lower. This pattern is consistent with the trend in the discrete measurements of stage data discussed in the section titled "Trends in Discrete Stage and Discharge Magnitudes." Based on visual inspection of the time series, the variability of stage values may be increasing with time.

There were 63 days where mean stage could not be computed from available unit value data, about 0.57 percent of the 10,957 days in the period of analysis. Of the days with missing stage, 58 were during rating 18 and 5 were during rating 19. The winter months of January and December had the highest number of missing stage data with 21 and 34 days, respectively. Some of the missing values during the winter months may reflect ice-backwater conditions when available stage data was not indicative of rated flow. Estimated daily mean flows were used with rating 18 flow-stage relation to inversely estimate all missing daily mean stage values.

Relation Between Discrete Stage Measurements and Daily Mean Stage

Figure 6 shows the correspondence between discrete stage on days of field measurements and daily mean stage computed from unit values on that day. Only one estimated stage occurred on a day of a discrete measurement. To model flows and track the changes in the stage-discharge relation, however, daily mean stages and flows were replaced with measured discrete stages and flows on days of field measurements. This replacement matched discrete measurements of stage and discharge, which were the basis for parameter estimation in the state-space model.

Frequency Density of Streamflow Data

Modeling approaches are commonly based on the normal probability density of model errors; however, the probability density of errors tends to have a similar shape as the probability density of the response variable. Here, the probability density of daily mean flows from the Pere Marquette streamgage were analyzed for the 30-year period for waters years 1990 through 2019. After a natural (base e) logarithm transformation of daily mean flows, a two-parameter normal and a three-parameter gamma distribution were fit (Delignette-Muller and Dutang, 2015) to the data (fig. 7). The resulting Akaike information criterion (AIC) for the two distribution functions were 9,106 and 8,249, respectively, indicating that the three-parameter gamma distribution (indicated by the smaller AIC value) was more likely to be the appropriate model. The estimated shape, scale, and threshold parameters for the gamma distribution were 7.5203, 0.1246, and 5.5833, respectively; thus, the gamma family of distributions was specified with a natural log link function in subsequent modeling of flows.

Stage and Discharge Relations

Stage-discharge rating tables 18–21 for the Pere Marquette streamgage were retrieved from USGS NWIS databases using Aquarius Time-Series Software (Aquatic Informatics, 2022). Table 2 shows the starting and ending dates for each of the selected ratings and the number of discharge measurements in the corresponding interval when the ratings were applied.

Figure 8 shows rating curves 18–21 applied from 1986 through 2019 with corresponding color-coded discrete measurements. The curves generally tend to shift to the right with time indicating that higher rates of discharge associated with the same stage. Ratings 18–21 were developed manually, and the ratings track changes closely. Ratings 18 and 21 are approximately parallel and indicate the left and right boundaries for rated discharges during the selected period of analysis, while ratings 19 and 20 are convergent with each other and with rating 18 at higher discharges.

Table 2. Selected rating periods for U.S. Geological Survey streamgage 04122500 Pere Marquette River at Scottville, Michigan.

Rating period			Number of discrete measurements
Rating number	Starting date	Ending date	
18	October 1, 1986	October 25, 1994	64
19	October 25, 1994	March 1, 2011	92
20	March 1, 2011	October 1, 2013	17
21	October 1, 2013	October 1, 2019	39

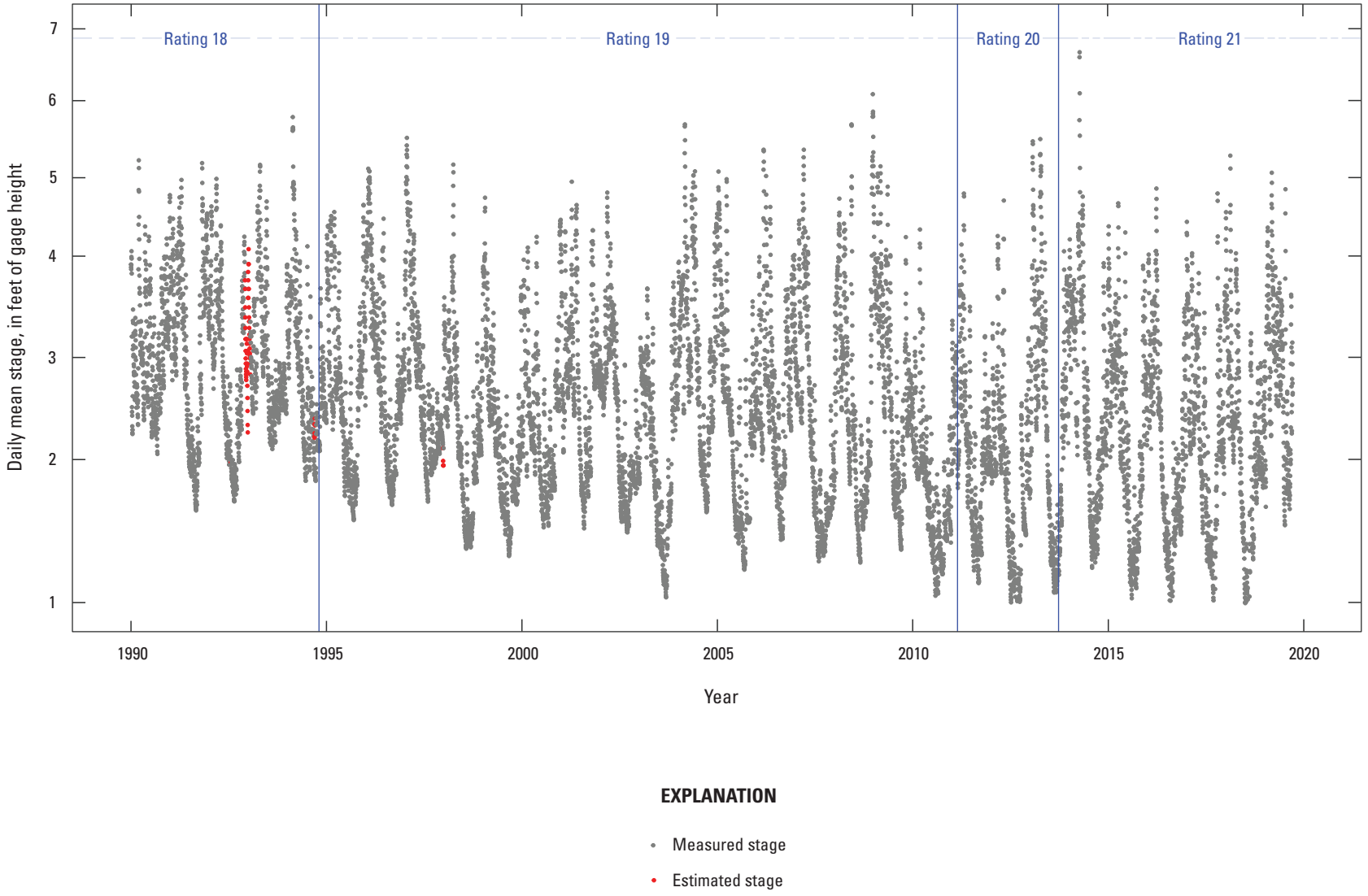

Figure 5. Measured and estimated daily mean stage at U.S. Geological Survey streamgage 04122500 Pere Marquette River at Scottville, Michigan.

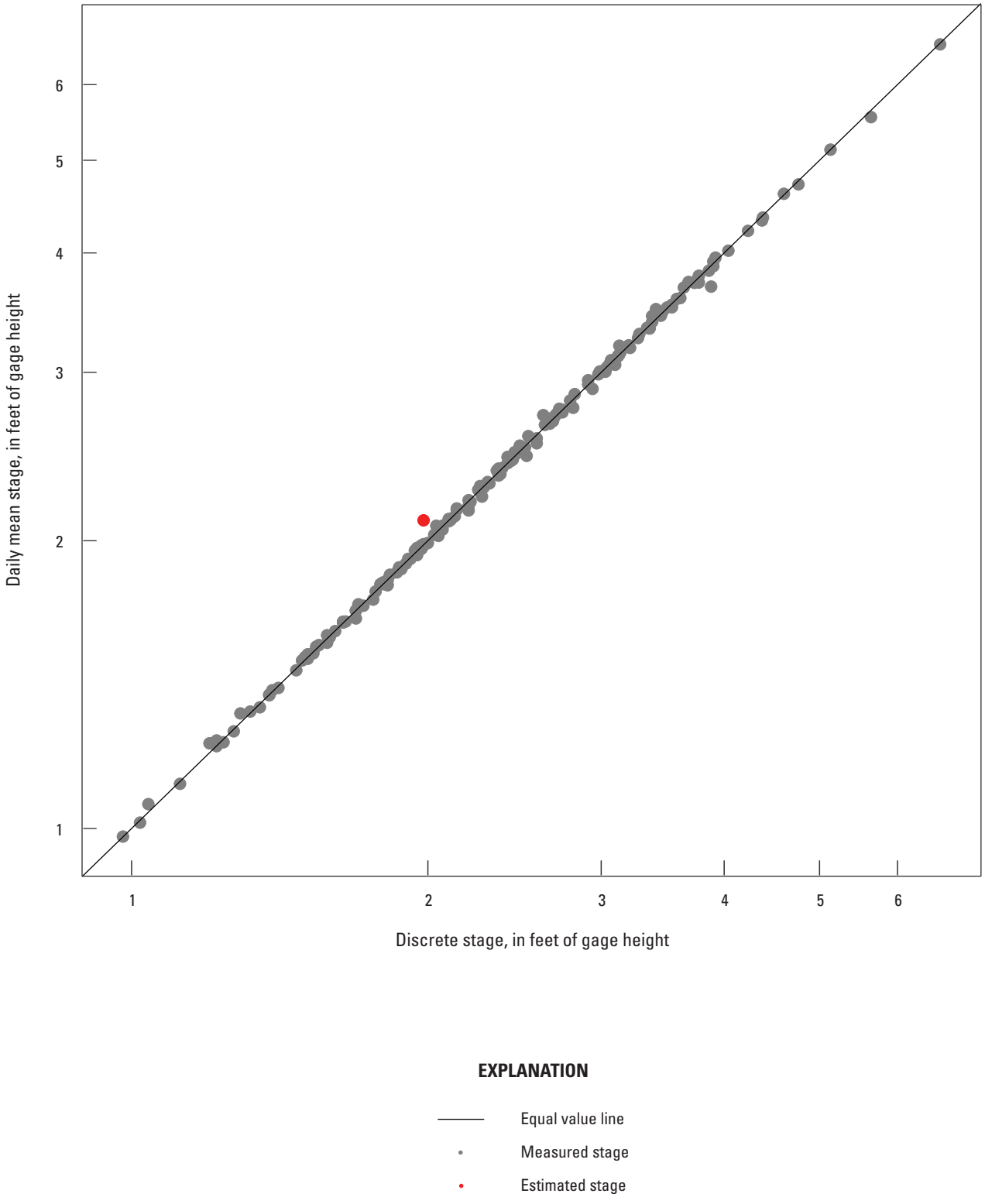

Figure 6. Relation between discrete stage and daily mean stage at U.S. Geological Survey streamgage 04122500 Pere Marquette River at Scottville, Michigan.

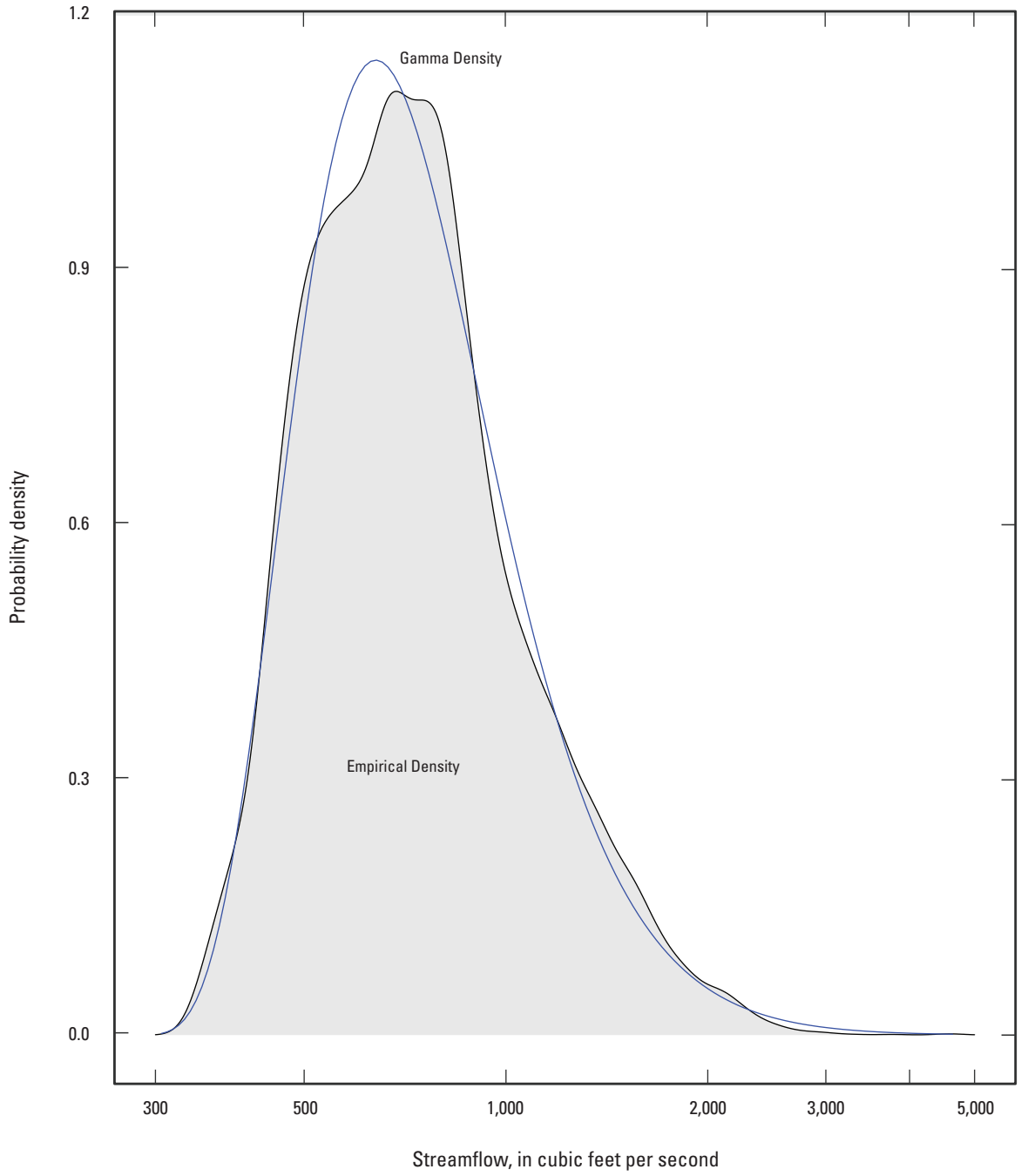

Figure 7. Probability density of daily mean flows at U.S. Geological Survey streamgage 04122500 Pere Marquette River at Scottville, Michigan, from water years 1990 to 2019.

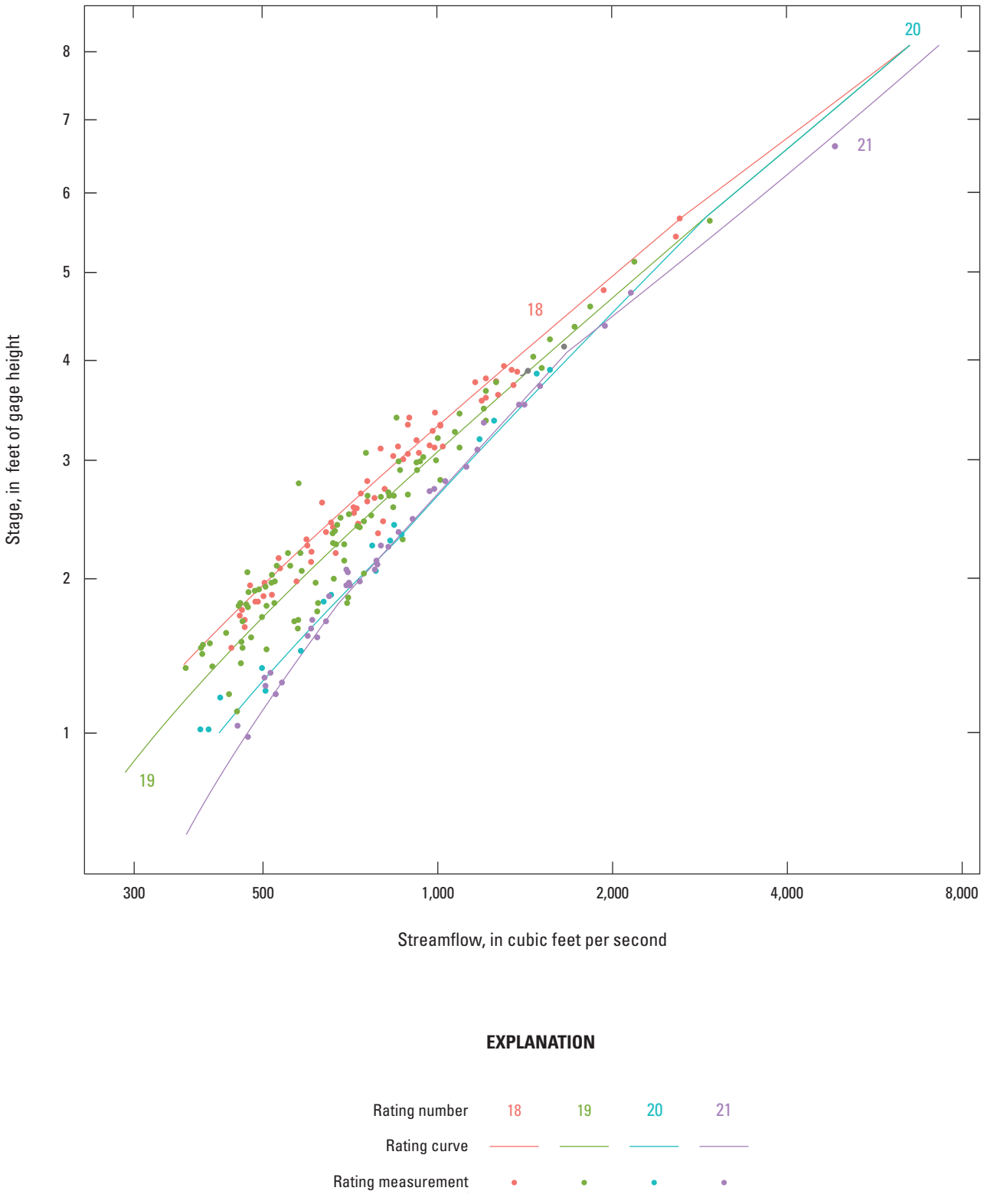

Figure 8. Discrete measurements with base rating curves for U.S. Geological Survey streamgage 04122500 Pere Marquette River at Scottville, Michigan.

Methods for Computer-Aided Adaptation of Stage-Discharge Ratings

A stage-discharge rating is described by a monotonically increasing set of ordered stage-discharge values that together approximate a curve. Unlike a smooth line defined by a continuous function, the stage-discharge rating may require interpolation of discharges between discretized stage values. This type of monotonic increasing rating is commonly used to compute discharge at streamgages that are not affected by variable backwater conditions such as tidal estuaries.

Methods for computer aided adaptation of ratings imply that an initial rating is available or is needed to initiate the process. For USGS streamgages, a set of discrete stage and discharge measurements are commonly available (or can be obtained) to characterize stage-discharge relations throughout the range of interest. Measurements can be selected from this set to represent a fairly time-invariant period of stage-discharge conditions from which to develop a corresponding rating. A rating table is a tabular form of the data that is graphically represented in a rating curve (Rantz, 1982b). A rating table may discretize stage at 0.1- to 1.0-ft intervals, depending on the linearity of the rating curve. An expanded rating table can be used to discretize the rating more finely at 0.01-ft intervals to approximate a rating curve more closely with areas of sharp curvature. To algorithmically adapt the rating, however, it is convenient to approximate a rating table with a parametric equation rather than a discretized table.

In the following section, the approximation of a rating by a parametric equation from an expanded rating table and a set of discrete measurements is developed and described. The parametric equation provides a basis for adapting the relation by changing five parameters.

Splines for Approximating Stage-discharge Ratings

Low-order polynomials are commonly used to approximate simple curvilinear relations but are particularly useful for approximating functions at a single point. When approximating functions across a wide domain (such as a stage-discharge rating), however, splines are preferred because they have favorable theoretic approximation properties (Wood, 2006, 2017). In particular, splines are less erratic in extrapolation than high order polynomials.

Like polynomials, splines use basis functions $\phi(x)$ for approximation; for example, basis functions for a simple linear polynomial regression include a basis function that produces an intercept term by mapping all values of the explanatory variable x to 1 ($_p\phi_0(x^0)\rightarrow 1$) and a second basis function that maps all values of x to itself ($_p\phi_1(x^1)\rightarrow x$). Basis functions for cubic regression splines (Wood, 2006, 2017) used in this report are a function of stage and knot locations $_s\phi$(*stage,knot locations*). Polynomials and splines provide a means for linear estimation as

$$\hat{y}_k = \sum_{i=0}^{p} \hat{\beta}_i \cdot \phi_i(x_k), \quad (1)$$

where

p is the number of basis functions used, and

$\hat{\beta}_i$ is and estimated parameter associate with the ith basis value.

For time varying ratings, the estimated parameters would be indexed by both i and k ,$\theta_{i,k}$ and may be referred to as a vector of hyperparameters.

Cubic regression splines (CRS) provide a single equation for computation of flows that is linear in parameters. This linearity implies that derivatives of the CRS with respect to any of the parameters are not a function of other parameters. These characteristics greatly simplify the sequential estimation of parameters controlling the local curvature of the CRS. In addition, CRS are constrained to linear extrapolation at the slopes defined at the end points of the curve, which are determined by the minimum and maximum stages used in developing the rating. Finally, the flexibility of CRS for closely approximating stage-discharge ratings can provide continuity in the transition from manual to computer-aided adaptation of rating curves.

Cubic Regression Spline Specification

CRS are formed by a set of piecewise cubic (third order) polynomials with constraints to ensure continuities of second-order derivatives at interior knots, which are stage values where adjacent polynomials intersect. Additionally, continuity of first-order derivatives is a constraint at the exterior knots (Wood, 2006, 2017). This constraint provides a basis for linear extrapolation at the slopes defined at the minimum and maximum values of stage measurements. The number of cubic polynomials is determined by the specified number of knots minus one.

In this analysis, CRS parameters were estimated within a Generalized Additive Modelling (GAM) framework to flexibly represent the monotonically increasing relation between stage and discharge. The GAM package mgcv (Wood, 2021) in R was used to develop the CRS, which provided penalties for overfitting, stage-dependent spline basis values, parameter estimates and uncertainties, and statistics on model fit (see Wood (2006, 2017) for details).

Within the R environment with the mgcv package, the syntax for estimation of CRS is

$$GAMobject \leftarrow gam(discharge \sim s[stage,\ bs = 'cr',\ knots = 5],\ data = rating18,\ family = Gamma[link = \log]) \quad , \tag{2}$$

where

rating18	is *discharge* and *stage* from the expanded table for rating 18;	
s[*stage*,…]	indicates that smoothing spline basis will be computed as a function of stage;	
bs	is the type of bases used, which was specified as '*cr*' for a cubic regression spline;	
knots	specify the number of knots in the spline;	
data	are the expanded (0.01 ft increment of stage) table for rating 18 at the Pere Marquette streamgage;	
family	indicates the distribution family that approximates *discharge*; and	
link	*log*	indicates that a natural logarithm function was used to transform *discharge.*

The number of knots was specified as 5 for all CRS developed in this report. The appropriate number of knots is streamgage and rating-curve dependent. Wood (2006, 2017) provides guidelines for fitting CRS.

Spline Parameters and Basis Values

Once the CRS is estimated, the spline parameters and basis values can be extracted from the *gamObject* (eq. 2). The scalar product of the spline parameter vector and the basis vector for a corresponding stage result in the CRS estimate of the logarithm of discharge.

The function **coefficients** with argument *gamObject* returns the parameter vector, $\hat{\beta}_{CRS}$, of length equal to the number of specified knots for the spline. By default, the two exterior knots were located at the minimum and maximum of the stage value in the rating table. The three interior knots are located at the lower, middle, and upper quartile of the stage values. Alternatively, interior knot locations can be specified to correspond to hydraulic breakpoints such as the elevation of riffle, channel, and overbank control transitions.

In figure 9, the first interior knot for rating 18 is at 3.075 ft of gage height (shown in orange) while the first interior knot for rating 21 is at 2.4225 ft of gage height (shown in purple), a difference of −0.6525 ft. The range of knot locations within each basis decreases with higher knot values because larger knot values (locations) commonly do not vary as much with time (or rating). Also, basis 1–4 have a mean of zero and generally have a range from [−1, 1] for all ratings. The basis 0 for all ratings is a constant value of 1, which is not plotted. The corresponding knot is located at the minimum stage. The maximum value of each basis 1–4 is at the stage for the corresponding knot, shown by the vertical lines.

The mgcv package provides two functions to extract or compute basis values with a *gamObject*. Once the number of knots is specified, the basis values for splines are strictly stage dependent, like the basis values for polynomials. Applying the function **model.matrix**(*gamObject*) will extract the sets of basis values for the stage measurements used in model development. Alternatively, basis values can be computed for any new set of measured stages by use of the function **predict.gam**(*gamObject*, newdata = data.frame(stage = [vector of unit or daily values of stage], type = 'lpmatrix') where the stage vector is included as a variable in the R environment. Output from these functions is an *nobs*×*knots* matrix that is used in the measurement array $\boldsymbol{Z}$ in measurement equation 4.

Discrete-Time State-Space Model

A state-space model consists of two equations: a state equation 3, and a measurement equation 4. As a Bayesian model, a specification of initial parameter magnitudes and uncertainties also is provided. The discrete-time state-space model form is presented here because stage measurements are obtained at unit (discrete) intervals and computations used in state-space modeling are made by use of discrete time steps. As a reminder of the discrete orientation, the time since the start of the computation is indexed by the symbol k, where k is an element of the whole numbers [0,1,2,…,T]. A value of k=0 indicates an initial condition for the computation at k=1; the maximum whole number used in computations is indicated as k=T, indicating the last time step in the period of analysis.

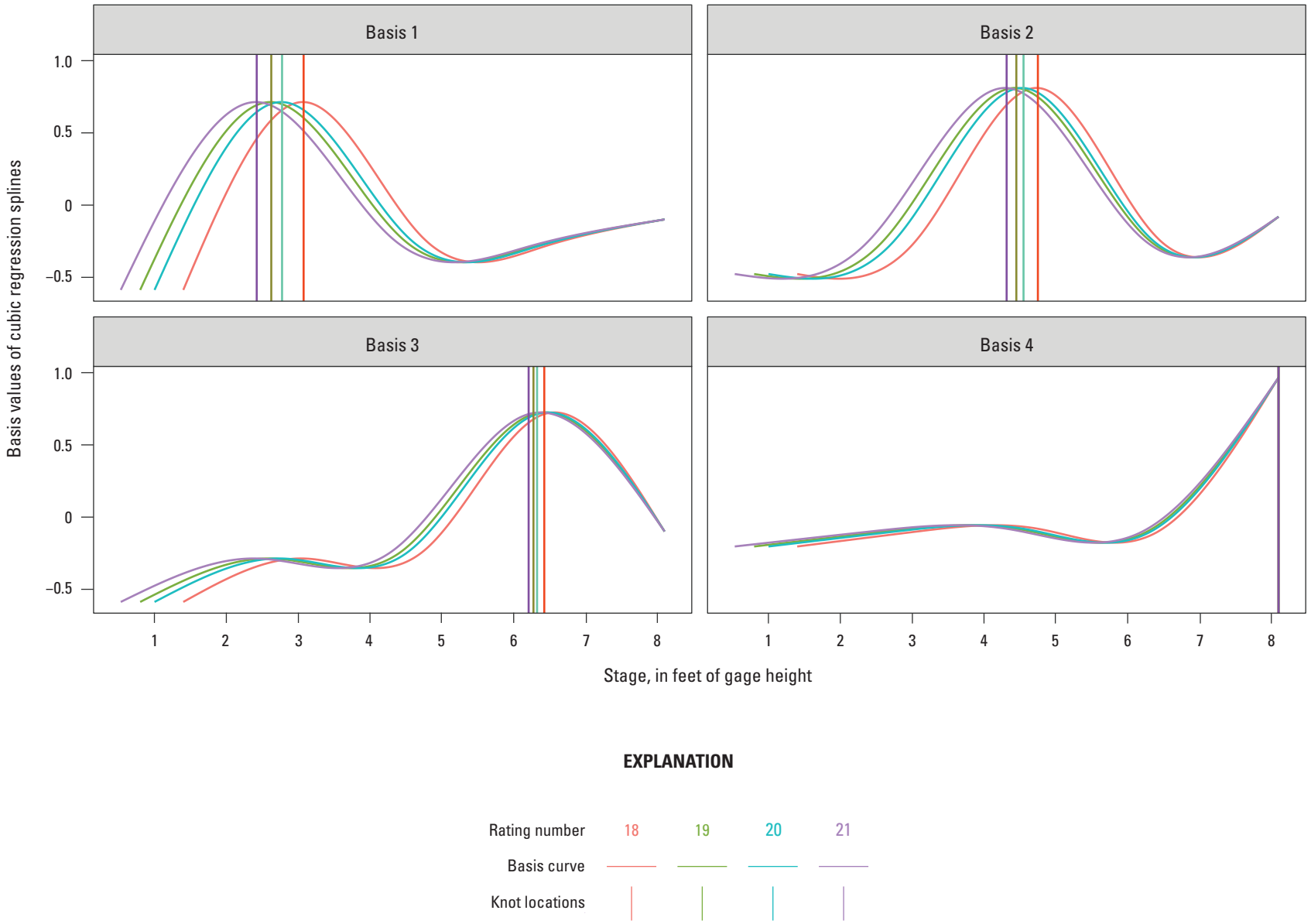

Figure 9. Basis values for cubic regression splines computed from rating curve tables at U.S. Geological Survey streamgage 04122500 Pere Marquette River at Scottville, Michigan.

State Equation: $\boldsymbol{x}_k = B \cdot \boldsymbol{x}_{k-1} + \boldsymbol{w}_{k-1}$, where $\boldsymbol{w}_{k-1} \sim N^m(0, Q_{[.,k,\Delta k]})$, (3)

where

$\boldsymbol{x}_{k-1}$ is the measurement-updated stat vector at time $k-1$ with elements in $\mathbb{R}^{m\times 1}$;

$\boldsymbol{x}_k$ is the temporally updated state vector at k;

B is the (time invariant) state transition matrix with elements in $\mathbb{R}^{m\times m}$;

$\boldsymbol{w}_{k-1}$ is the state-error vector at $k-1$ with elements in $\mathbb{R}^{m\times 1}$ that are multivariate normally distributed with dimension m, N^m; and

Q is the process error covariance matrix with element in $\mathbb{R}^{m\times m}$. It can be time invariant (without subscripts), vary with time, Q_k, or vary with time step length, $Q_{\Delta k}$.

Measurement Equation: $y_k = \boldsymbol{Z}_{n,m,k} \cdot x_k + v_k$, where $v_k \sim N^n(0, R_k)$, (4)

where

y_k is a scalar time series of the natural logarithms of discrete flow measurements, when available, and *not available* (*NA*) indicator for missing values;

$\boldsymbol{Z}_{n,m,k}$ is the design array of basis vectors with elements in $\mathbb{R}^{n\times m\times T}$;

T is the length of the period of analysis, in time steps;

v_k is the unknown scalar measurement error with a multivariate normal distribution with dimension n, N^n; and

R_k is the measurement error variance at k, which may be a constant.

Initial Conditions for the state vector: $x_0 \sim N^m(\mathrm{E}[x_0], \mathrm{var}[x_0])$, (5)

where

N^m indicates the multivariate normal distribution with the dimension m,

$\mathrm{E}[x_0]$ is the expected value of the initial state vector, and

$\mathrm{var}[x_0]$ is the $m\times m$ state error covariance matrix.

The state and measurement equations are evaluated alternately at each time step and are discussed in the context of adaptive ratings and streamflow uncertainty in the following sections.

In this report, the time series for the state vector receive measurement updates when discrete measurements are available. Initial conditions are specified for the state vector (eq. 5), where x_k represents the temporal changes in each of the five spline parameters as indexed by k. Because the state vector explicitly represents time varying parameters, the more specific and descriptive term "hyperparameter vector" or just "hyperparameters" is used instead of the term "state vector" for greater clarity depending on the context.

Implementation of the state-space model described in this report was made possible by the Multivariate Auto-Regressive State-Space (MARSS) package developed by Holmes and others (2020a). The package is freely available and runs in the R language and statistical computing environment. To facilitate cross referencing, the notation used in this report is generally consistent with the MARSS user guide (Holmes and others, 2020b) and Shumway and Stoffer (2016). In particular, the interested reader may wish to reference these guides to further clarify and extend their understanding of the symbology and **text shortcuts** for common structures describing the transition matrix B and process and measurement error covariance matrices Q and R, respectively.

State Equation

Within the state equation, premultiplying the m-dimensional state vector x_{k-1} by the $m\times m$ state transition matrix B forecasts the state vector to time k. In general, elements of B may be fully specified or estimated using the MARSS software if the eigenvalues fall within the unit circle (Holmes and others, 2020b). For cases where the parameters may drift without necessarily reverting to a mean, the transitions can be modeled as a random walk by specifying B as an identity matrix. A random walk was selected here to describe these transitions because of the monotonic trend in the discrete stage values (fig. 2) did not appear to revert to a mean. Selection of the structure for the B matrix is a streamgage-specific determination.

The time varying elements of the process error vector w_{k-1} are unknown but are statistically characterized as vectors with a multivariate normal distribution having an expected value of zero and covariance Q, which is referred to as the process-error covariance matrix. This matrix describes the incremental increase in uncertainty of the state-error covariance matrix P with each forecast (temporal) update of the state vector containing the hyperparameters for the CRS (see Simon [2006] for details). In this report, the Q matrix was time invariant because the discrete measurements were not considered to be sufficiently frequent to characterize possible time varying errors during the transition from open-water to ice-affected streamflow conditions when flows are more commonly estimated at this streamgage.

More generally, the notation Q_k or $Q_{\Delta k}$ indicates that Q can vary with time index k or with the length of the time step Δk. In particular, periods of greater and lesser hyperparameter variability can be accommodated by changes in the magnitudes of elements in the process-error covariance matrix; for example, greater hyperparameter variability and process error covariance magnitudes may be

associated with the rapid onset and dissipation of changes in the stage-discharge relation because of variable ice effects. In this report, however, Q is simply modelled at a fixed $Q_{\Delta k}$ of daily values. The following discussion is provided to describe how the estimated value of $\hat{Q}_{\Delta k}$ can be adjusted to accommodate a different time step $\Delta k' < \Delta k$ than the one used to estimate the state-space model parameters.

The process error covariance matrix Q was estimated at daily time steps because of the extended (30-year) period of analysis and the relatively sparse discrete measurements (one discrete measurement on average every 56.9 days). In addition, the estimation process is computationally intensive when tracking time-varying state-space model parameters. Refining the time step would not have improved the understanding of the timing of hydraulic control changes but would have substantially increased the computational requirements. Addition of unit flow information in the measurement time vector y_k from the streamgaging network, however, may support refinement of the timing of shifts and justify additional computational efforts for shorter periods of analysis.

Simon (2006) justifies rescaling the process covariance error with the argument that any discrete-time process covariance Q_k divided by the length of the time step Δt is approximately equal to the continuous-time process covariance at time k as $Q_c(t_k)$ for

$$\frac{Q_k}{\Delta t} \approx Q_c(t_k) \text{ for small } \Delta t. \tag{6}$$

Analogous to equation 6, it is argued here that we can simply rescale $\hat{Q}_{\Delta k}$ for different discrete time intervals as

$$\frac{\widehat{Q}_{\Delta k}}{\Delta k} \approx \frac{\widehat{Q}_{\Delta k'}}{\Delta k'} \text{ for small } \Delta k. \tag{7}$$

For example, if $\hat{Q}_{\Delta k}$ is a 5×5 identity matrix, with Δk=1,440 minutes (min) (daily time step) and $\Delta k'$=15 min, then the diagonal elements of $\hat{Q}_{\Delta k}$ would equal 15/1,400.

This assumption allows for the efficient estimation of Q, which also may improve the numerical stability of the estimate of Q as these elements are generally small values bounded below by zero. This also provides flexibility for application to periods when the lengths of unit time intervals differ (fig. 4).

Once the form of the state-space equation is identified and associated parameters are estimated, Kalman filtering and smoothing may be applied to the computation of unit discharge magnitudes and uncertainties at time steps different from those used to estimate parameters of the state-space model using equation 7. In the engineering and statistical literature, the term filtered refers to estimates of flow based on data before or concurrent with the time for which flow is estimated (Shumway and Stoffer, 2016). Filtered estimates of flow can be made available in real time. The term smoothed refers to estimates of flow using data before and after the time for which flow is estimated. Smoothed estimates may be more precise than filtered estimates because they are delayed from the time of estimation, providing more time for additional data to become available.

Alternate forms of the process error covariance Q matrix were estimated within the MARSS package (Holmes and others, 2020a). All covariance matrices need to be symmetrical and positive definite. Common forms are identified by tags to facilitate applications. These include (1) "**diagonal and equal**," which implies a diagonal matrix with equal variance components; (2) "**diagonal and unequal**," which implies a diagonal matrix with unequal variance terms; (3) "**equalvarcov**," which implies a symmetrical matrix where the variances are equal to each other and the covariance or off diagonal terms are all equal to each other; (4) "**unconstrained**," which implies a matrix where variances and covariance may differ, but symmetry and positive definiteness is maintained; (5) a "**zero**" matrix; and (6) an "**identity**" matrix.

Initializing the State Vector

The initial state vector is assumed to be normally distributed as $x_0 \sim N^5(\mathrm{E}[\beta'_{CRS}], \mathrm{var}[\beta'_{CRS}])$; thus, the initial estimate for $x_0^+ = \beta'_{CRS}$, which corresponds to the spline parameters in the 5-knot CRS estimated using data from rating table 18. As indicated previously, the parameter variance is underestimated from rating table data, so the initial state error covariance matrix was multiplied by 1,000, $P_0^+ \leftarrow 1{,}000 \text{ var } (\beta'_{CRS})$ to help compensate for the rating table's lack of measurement variability. The effect of the multiplier is to allow the state vector (hyperparameters) to vary more quickly with subsequent discrete measurements.

Measurement Equation

In the measurement equation 4, the forecast state vector x_k is premultiplied by the kth row vector from the design array $\boldsymbol{Z}_{l,\cdot,k}$. This scalar product is the state-space model estimate of the natural logarithm of flow at time k. When the measurement vector y_k contains a value of discharge, the state-error covariance matrix is updated, which generally reduces the uncertainty of the state vector depending on the measurement variance R_k. If no measurement information is available at time k, the discharge estimate is computed but the state-error covariance matrix is not updated (reduced) from the forecast update.

Measurement Time Series of Discrete Discharges

The scalar measurement time series y_k has a length equal to the number of days in the 30-year period of analysis. On days of discrete measurements, the series contains the natural logarithms of measured discharges in cubic feet per second. Otherwise, y_k is assigned a missing value

indicator of *NA*, which is interpreted as "not available" in the R programming environment. About 98.3 percent of the elements of y_k were assigned *NA* status in this analysis.

In a network formulation, however, time steps without discrete measurements could contain a regression estimate of discharge based on discharges at nearby streamgages, with a corresponding prediction variance included in the measurement error variance matrix R_k. Strategic placement of regression estimates at times of the onset or dissipation of ice-effects, for example, with corresponding increases in the error covariance matrix Q_k may facilitate the rapid adaptation of the rating to ice-affected conditions even when discrete measurements are relatively sparse.

Design Array

The design array $\boldsymbol{Z}$ contains the basis vectors computed using the stage time series data and the CRS knot specifications. Basis vectors can be computed for any set of stage values by use of the fitted *gamObject* returned in the CRS development. The four following steps outline the computation of the basis vectors in R:

Algorithm 1. Computing basis vectors for stage values from a GAM object

1. Use the *predict* function in *mgcv* to compute basis vectors from stage time-series data and specified knot locations, Z = *predict*(gamObject, newdata = data. frame(stage= stage_time_series), type = 'lpmatrix').
2. Transpose the Z matrix with the R function t as $Z = t(Z)$.
3. Remove row names from the matrix Z as rownames(Z) = *NULL*.
4. Convert the Z matrix to the array $\boldsymbol{Z}$ by use of the R *array* function $\boldsymbol{Z}$ = *array*(Z, *dim*(n,m,T)).

Measurement Error Variance

As the MARSS package is applied in this report, it is assumed that the measurement errors of the natural logarithms of discrete discharges are about normally distributed and unbiased (mean zero) with variance, R_k, and may be time dependent as $v_k \sim N(0,R_k)$. There are many variables that can affect the accuracy of a discharge measurement including the type and condition of equipment used, the characteristics of the discharge measurement section, how rapidly the stage is changing during the discharge measurement, the presence of ice or debris, other environmental conditions during the measurement, and the experience and subjective evaluation by the hydrographer making the measurement (Rantz, 1982b). The difficulty in quantifying the uncertainty in the field is related to subjectively and consistently assessing the accuracy of the measurement at a wide variety of streamgages, channel, discharge conditions, and hydrographers.

Measurement variances were either specified using field-based measurement qualifiers or estimated as an unknown constant using the "**diagonal and equal**" tag. Frequencies of the measurement qualifiers of Excellent, Good, Fair, or Poor (table 1) varied among the four corresponding categories from about 92 percent for Good measurements to 0 percent for Excellent measurements. All three measurements rated Poor in table 1 were associated with ice-affected discharge conditions and were removed from this analysis. Given this distribution inequality of qualifiers among categories, estimation of a factor variable with four discharge accuracy qualifier levels was infeasible. Instead, the four qualifiers of Excellent, Good, Fair, and Poor were assigned percent errors of 2-, 5-, 8-, or 12-percent (U.S. Geological Survey, 2011). Because these percent errors were relatively small, they are approximately equal to the standard errors of the natural logarithms of discharges. So, measurement variances were computed and assigned to each discrete discharge measurement as 0.02^2, 0.05^2, 0.08^2, and 0.12^2, respectively, to form a time "**series specified variance**." Finally, the average of the measurement variances was computed and assigned to discrete measurements as a constant "**mean specified variance**."

For time steps when discrete measurements were available, a measurement update was applied to the state-error covariance matrix as

$$P_k^+ = \left[(P_k^-)^{-1} + Z'_{1,.,k} \cdot R_k^{-1} \cdot Z_{1,.,k}\right]^{-1}, \quad (10)$$

which results in a decrease in the uncertainty of the state vector. For time steps without a discrete measurement, the state-error covariance matrix was set to the state updated covariance $P_k^+ \leftarrow P_k^-$.

Methods for Computing Magnitudes and Uncertainties of Unit Discharges

Computing estimates of discharge magnitudes (and their corresponding uncertainties) is a function of how the timing of the point of estimation k compares with the interval of available data, $y_{1:s}=\{y_1, y_2,\ldots, y_s\}$. This section provides a general outline on how the temporal and measurement updates to the state vector x, the state-error covariance matrix P, and the innovations variance series $\sum$ are applied, and how the covariance matrices are used to compute uncertainties of elements in the state vector and discharges are computed in the context of Kalman filtering and smoothing.

Kalman Filtering

Kalman filtering uses discrete measurement data before and at the current time step k if they are available; thus, for streamgages that have telemetry to transmit real-time stage data, Kalman filtering can be used to compute real-time estimates of the magnitude and uncertainty of discharge. Notation used in this report is generally consistent with Holmes and others (2020b) and Shumway and Stoffer (2016) who provide additional details and discussion.

Here, a temporal update of the state vector to time indexed by k is obtained by premultiplying the state vector at $k-1$ by the transition matrix B (eq. 11). Note, the "+" superscript on the right-hand side of equation 11 indicates that the state vector at $k-1$ may have received a measurement update if a discrete measurement was available at $k-1$. The "–" superscript on the left-hand side indicates a measurement update has not yet been applied to the state vector at time k.

The transition matrix B may take different forms. In this report, the stage required to pass most discharges generally decreased with time. Thus, the corresponding hyperparameters (state vector) describing this type of change were also expected to drift systematically with time. This type of transition is commonly associated with a random walk, which is modelled using an identity matrix to represent the transition matrix. Without the systematic trend, an autoregressive form for the transition matrix may have been more appropriate.

$$x_k^- = B \cdot x_{k-1}^+. \tag{11}$$

Similarly, the temporal update to the state-error covariance matrix, before the measurement at time k, is incremented by the process-error covariance matrix as

$$P_k^- = B \cdot P_{k-1}^+ \cdot B' + Q_{k|\Delta k}. \tag{12}$$

When a discrete measurement of discharge (y_k) is taken at time k, a post measurement update for the state vector is computed as

$$x_k^+ = x_k^- + K_k(y_k - Z_{1,\cdot,k} \cdot x_k^-). \tag{13}$$

To facilitate the update, the Kalman gain matrix at time step k (K_k) is precomputed as

$$K_k = P_k^- \cdot Z'_{1,\cdot,k} \left[Z_{1,\cdot,k} \cdot P_k^- \cdot Z'_{1,\cdot,k} + R\right]^{-1}. \tag{14}$$

If no discrete discharge measurement is available at time k, then $x_k^+ \leftarrow x_k^-$. Likewise, if a discrete discharge measurement is available, the post measurement update to the state-error covariance matrix is computed as

$$P_k^+ = \left[I - K_k \cdot Z_{1,\cdot,k}\right] \cdot P_k^-, \tag{15}$$

where

I is a 5×5 identity matrix.

Without a discrete measurement, the state-error covariance matrix is updated as $P_k^+ \leftarrow P_k^-$. The diagonal components of P_k^+ can be used to estimate credible intervals about the state estimates (hyperparameters).

The predicted estimate of the logarithm of discharge at time k is

$$\hat{y}_k^- = \mathrm{E}\left[y_k \middle| y_{1:k-1}\right] = Z_{1,\cdot,k} \cdot x_k^-, \tag{16}$$

and the filtered estimate of the logarithm of discharge at time k is

$$\hat{y}_k^+ = \mathrm{E}\left[y_k \middle| y_{1:k}\right] = Z_{1,\cdot,k} \cdot x_k^+. \tag{17}$$

The filtered innovations time series—the unexplained deviations from the logarithm of discharge—are computed as

$$v_k = y_k - \hat{y}_k^+. \tag{18}$$

The filtered innovation covariance time series matrix is computed as

$$\Sigma_k^+ = Z_{1,\cdot,k} \cdot P_k^+ \cdot Z'_{1,\cdot,k} + R_k. \tag{19}$$

The innovation variance is used to compute credible intervals about the discharge estimates.

Kalman Smoothing

Kalman smoothing updates Kalman filter estimates within an interval that starts and ends with discrete flow measurements. The inclusion of flow information after the time step being estimated delays the availability of discharge information but may provide improved accuracy by utilizing post-time-step data. Initial Kalman state smoother estimates ${}_sx$ are based on updated Kalman filter estimates at the end of the estimation interval as ${}_sx_T = x_T^+$. Smoothing computations progress backward through time from $k=T,T-1,\ldots,1$. Previously computed Kalman filter states and state error covariance matrices P also are reused in the computation of the smoothed estimates.

The initial smoothed state and state-error covariance matrix estimates (designated ${}_sx_T$ and ${}_sP_T$) are computed as

$${}_sJ_k = P_k^+ \cdot B' \cdot \left[P_{k+1}^-\right]^{-1}, \tag{20}$$

$${}_sx_k = x_k^+ + {}_sJ_k({}_sx_{k+1} - x_{k+1}^-), \text{ and} \tag{21}$$

$${}_sP_k = P_k^+ + {}_sJ_k({}_sP_{k+1} - P_{k+1}^-)\,{}_sJ'_k. \tag{22}$$

The smoothed estimate of the logarithm of discharge at time k,

$$ {}_s\hat{y}_k = \boldsymbol{Z}_{1,\cdot,k} \cdot {}_s\boldsymbol{x}_k. \quad (23) $$

A possible difficulty with smoothing is that change detected in the postdated information may not yet be relevant to the earlier time to which it is being applied. A time series may be especially sensitive to this difficulty if a rare event, such as a flood, causes a large change in hydraulic conditions after the time step being estimated.

Results and Discussion

Using data for the Pere Marquette streamgage, this section presents results for and discusses the uses of CRS developed from ratings and discrete measurements, the development and selection of a state-space model, a discussion of the state estimates or hyperparameters, the effects of hyperparameters on the stage-discharge rating, and the magnitudes and uncertainties of daily streamflow data.

Cubic Regression Splines

GAM was used to develop CRS models describing the relations between stage and discharge for the Pere Marquette streamgage for rating periods 18, 19, 20, and 21. CRSs were developed directly from ratings and from paired discrete measurements of stage and discharge obtained during periods when the ratings were effective. Both methods produced close approximations of the existing rating curves, but each method has advantages and disadvantages.

In the four stage-discharge ratings tested for Pere Marquette streamgage, this fit was almost exact (coefficient of determination: $r^2 \approx 1$; table 3). Each of these models included five degrees of freedom, corresponding to 5 knot CRSs, as indicated by the difference between the number of data points and the residual degrees of freedom. This goodness of fit implies a seamless transition between discharges computed by the manual rating and initial discharges computed by the state-space model.

The disadvantage of fitting the rating is that the rating table data do not indicate measurement variability, and the specified number of data points is somewhat arbitrarily based on the discretization of the stage data. In this report, an expanded rating was used that discretized the stage at 0.01-ft intervals, which for rating 18 corresponds to 671 data points. Had at 0.02- or 0.10-ft discretizations been used instead, there would have been about half to a tenth of the number of data points with little change in the regularity of the curve.

So, absent the measurement variability and the (high) arbitrary residual degrees of freedom, the covariance of the spline parameters is considered unreliable and almost certainly too small. The difficulty with an underestimated covariance matrix for the state space model is that the parameters in the state vector are indicated as being known to a higher precision than they are actually known. Therefore, the parameters are less sensitive (change less) in response to measurement deviances from the rating, causing the hyperparameters (and the rating) to adapt more slowly to subsequent discrete measurement information indicating needed changes to the rating.

Alternatively, the discrete discharge measurements can be used with a CRS to approximate the corresponding rating. The advantage of using the discrete measurements is that the covariance matrix of spline parameters will more

Table 3. Summary statistics for five-knot cubic regression splines for rating periods 18–21 at U.S. Geological Survey streamgage 04122500 Pere Marquette River at Scottville, Michigan.

Rating number	Number of data points	Residual degrees of freedom	Spline parameters					Coefficient of determination
			β_0	β_1	β_2	β_3	β_4	
Based on stage-discharge rating table								
18	671	666	7.4630	0.0879	0.6683	1.4662	1.5875	1.0000
19	731	726	7.4110	0.1233	0.7725	1.6162	1.6637	1.0000
20	711	706	7.5510	0.1302	0.6416	1.3788	1.4894	0.9999
21	758	753	7.5100	0.0540	0.6500	1.5489	1.6505	0.9999
Based on discrete stage-discharge measurement								
18	64	60.9	6.7270	0.0009	−0.0507	0.7022	2.1081	0.9927
19	92	90.0	6.5530	0.0929	0.0656	0.6087	1.4973	0.9582
20	17	13.5	6.5970	−0.0816	0.2736	0.4306	0.8894	0.9934
21	39	35.8	6.7770	−0.0518	−0.1113	0.5809	1.7735	0.9988
Period of analysis	222	220.0	6.6700	0.1196	0.0327	0.7363	2.3285	0.9494

accurately reflect the true uncertainty of the spline parameters. The corresponding disadvantage is that even if the same discrete measurements are used in the manual fit and the CRS fit, the shapes of the ratings may differ in minor ways; thus, a seamless transition between the manual rating and the initial state-space rating is not assured. Furthermore, the full spline covariance matrix is strictly applicable only if a full process error covariance matrix Q is specified. In any case, the structure of the state error covariance matrix P in the state-space model, and Q need to be consistent; for example, both might be specified as diagonal if the off-diagonal covariance elements are relatively small.

One strategy to ensure a seamless transition from an existing rating to an adaptive rating is to fit a CRS to the rating table of interest and use this parameterization to initialize the state vector $x_0^+ = \beta_{CRS}$ in the state-space model. The MARSS software can estimate the covariance matrix of the initial state vector $\hat{P}_0^+$, that is compatible with the structure of the specified Q matrix. Alternatively, the elements of the spline covariance matrix derived from fitting the rating can be inflated to approximate the estimated terms more closely. In this report, elements in the spline covariance matrix fitted to the ratings were multiplied by 1,000 to more closely approximate the covariance estimated by use of the discrete measurements.

The mgcv function **vcov**(*gamObject*) was used to extract the error covariance matrix of spline parameters in the CRS developed from expanded rating 18 for the initial state vector (Maechler, 2021). The covariance elements have low magnitudes (table 4) because most of the variation in rating 18 stage-discharge pairs is explained by the model. The correlation matrix was formed from the covariance matrix to illustrate the relatively low absolute value of correlations among spline parameters. These correlations are sufficiently low that problems associated with multicollinearity are considered unlikely.

Figure 10 shows the CRS stage-discharge base ratings for periods 18–21 along with 95-percent confidence intervals based on the discrete measurements obtained during the rating period. The corresponding expanded rating is shown for comparison. The CRS and expanded ratings are generally consistent for each rating period despite that CRS ratings are based only on discrete discharge measurements within the rating period. The widening CRS confidence intervals at higher stages show the utility of discrete measurements in reducing the uncertainty of the relation. The results support the use of the CRS approach for estimating ratings from data in a rating table or directly from discrete measurement data.

State-Space Modeling

Modeling results include the selection of the state-space model form, the depiction of changes in the state (hyperparameters) with time, the effect of parameter changes on the shape and fit of the stage-discharge relation indicated by the CRS, and the estimation of magnitude and uncertainty of discharge records.

Table 4. Initial state vector estimate based on spline parameters for expanded stage-discharge rating 18 at U.S. Geological Survey streamgage 04122500 Pere Marquette River at Scottville, Michigan.

[β_x, spline parameters estimated by use of rating 18; --, not applicable]

Estimates	Initial state vector parameters from rating 18				
	β_0	β_1	β_2	β_3	β_4
Mean vector					
--	7.4626	0.0879	0.6683	1.4662	1.5875
Covariance matrix					
β_0	1.916E−08	1.916E−23	1.583E−23	2.701E−23	−1.273E−23
β_1	1.916E−23	2.165E−07	4.938E−08	1.115E−07	1.221E−09
β_2	1.583E−23	4.938E−08	1.119E−07	3.309E−08	2.491E−08
β_3	2.701E−23	1.115E−07	3.309E−08	1.764E−07	−4.683E−08
β_4	−1.273E−23	1.221E−09	2.491E−08	−4.683E−08	2.974E−07
Correlation matrix					
β_0	1.0000	0.0000	0.0000	0.0000	0.0000
β_1	0.0000	1.0000	0.3174	0.5708	0.0048
β_2	0.0000	0.3174	1.0000	0.2356	0.1366
β_3	0.0000	0.5708	0.2356	1.0000	−0.2045
β_4	0.0000	0.0048	0.1366	−0.2045	1.0000

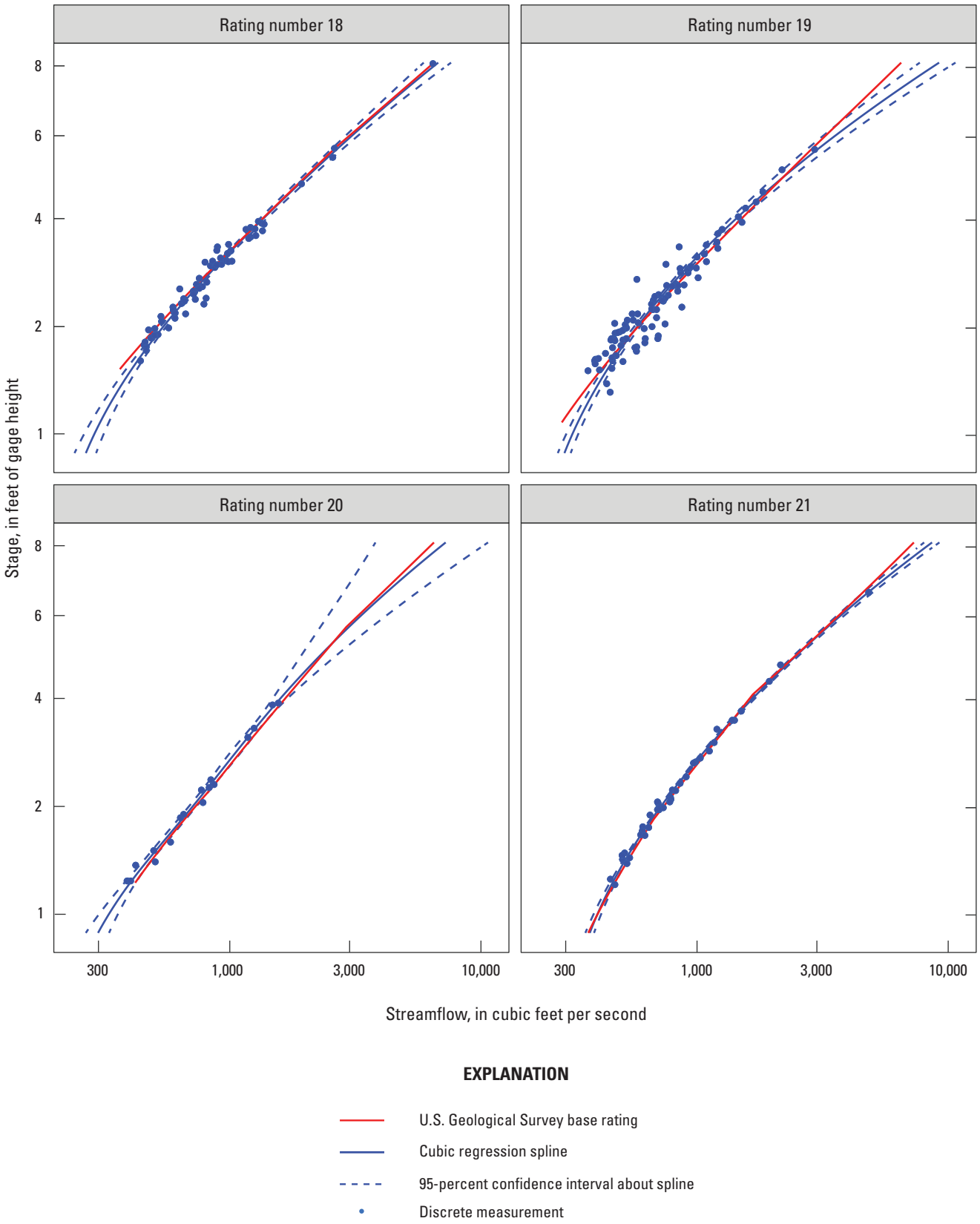

Figure 10. Rated discharge curve with cubic regression spline estimates of the magnitude and uncertainty of the rating based on discrete discharge measurements for U.S. Geological Survey streamgage 04122500 Pere Marquette River at Scottville, Michigan.

Table 5. Alternative state-space models developed for adaptive ratings at U.S. Geological Survey streamgage 04122500 Pere Marquette River at Scottville, Michigan.

[log -likelihood, a goodness of fit statistic that is maximized in model selection; AIC, Akaike information criteria is a measure of out-of-sample prediction error that is minimized in model selection; SE Qualifier, standard error of measurement qualifier, in percent, Excellent = 2 percent, Good = 5 percent, Fair = 8 percent, and Poor = 12 percent; Process variance Q estimated as 5×5 diagonal matrix with equal variances; BFGS, Broyden–Fletcher–Goldfarb–Shanno quasi Newton parameter estimation algorithm; kem, kernelized expectation-maximization algorithm for parameter estimation]

Model number	Form of process variance, Q	Form of measurement variance, R	Estimation method	Standard deviation		Log likelihood	Akaike information criteria	Number of parameters	
				$\sqrt{Q}$	$\sqrt{R}$			Q	R
1	Diagonal and equal	Diagonal and equal	BFGS	0.00153	0.07928	190.0	−376.0	1	1
2	Unconstrained	Mean specified variance	BFGS	0.02771	--	214.0	−398.0	15	0
3	Equalvarcov	Mean specified variance	kem	0.00226	--	209.7	−415.3	2	0
4	Diagonal and equal	Mean specified variance	BFGS	0.00158	--	211.4	−420.9	1	0
5	Diagonal and unequal	Diagonal and equal	BFGS	0.00051	0.07875	218.0	−423.9	5	1
6	Diagonal and equal	Series specified variance	kem	0.00180	--	233.4	−464.9	1	0

Development of State-Space Models

Table 5 lists alternative forms of the state-space model that were estimated sorted by decreasing AIC values, which balances the relative amount of information lost by overfitting and underfitting. Thus, the model with the smallest AIC statistic is preferred from a statistical perspective. The models differ structurally in the specifications of the time invariant process error covariance matrix Q and the estimated or specified scalar or time-varying measurement variance R. The AIC statistic is computed as AIC=2m−2 log(likelihood), where m is the length of the state vector and log-likelihood is the logarithm of the computed likelihood of the model given the data. Model 6, which has a single parameter that makes up the diagonal elements of the Q matrix and the lowest AIC value was selected to illustrate the results of the modeling approach.

Within MARSS, the Broyden-Fletcher-Goldfarb-Shanno (more commonly known as BFGS) algorithm provided much faster parameter estimation than the kernelized expectation maximization (more commonly known as kem) algorithm. The kem algorithm results in much slower parameter converge than the BFGS algorithm but provided more flexibility in the types of models estimated. Parameters forming the diagonal of the Q matrix were generally small values and bounded below by zero, which may have slowed convergence in some cases. Streamgages with more stable ratings are likely to have smaller values of Q.

Changes in Hyperparameters of Cubic Regression Spline

Figure 11 shows the time series of Kalman filtered and smoothed estimates of hyperparameters of the cubic regression spline computed in the development of state-space model 6. Times of discrete measurements are indicated by vertical grey lines. Note that the filtered estimates, which are computed forward through time, are shown as a step plot (horizontal lines between measurements and vertical lines at measurements) because filtered estimates only change at times of discrete measurements. In contrast, the smoothed estimates, which begin at the last filtered estimate and are computed backward through time, using filtered estimates in the computation. Thus, the smoothed estimates change more linearly between measurements because information before and after the time of estimation are used in the computation.

Note that filtered and smoothed estimates converge at the beginning and ending points of the time series. A lagged response is more evident between filtered and smoothed estimates for some parameters like β_3 and β_4 than others like β_0 and β_1. This lag may be associated with fewer discrete discharge measurements proximate to the higher stage knot locations associated with these parameters or with lower sensitivity of the parameter to discrete measurement data.

The results on figure 11 provide positive and negative support for a localized effect of a discrete measurements on model hyperparameters. Basis values vary with stage and are maximum at knot locations (fig. 9). Values of basis 1–4 are multiplied by corresponding states $\beta_1 - \beta_4$ and added to β_0 to estimate (the logarithm) of discharge. Positive support

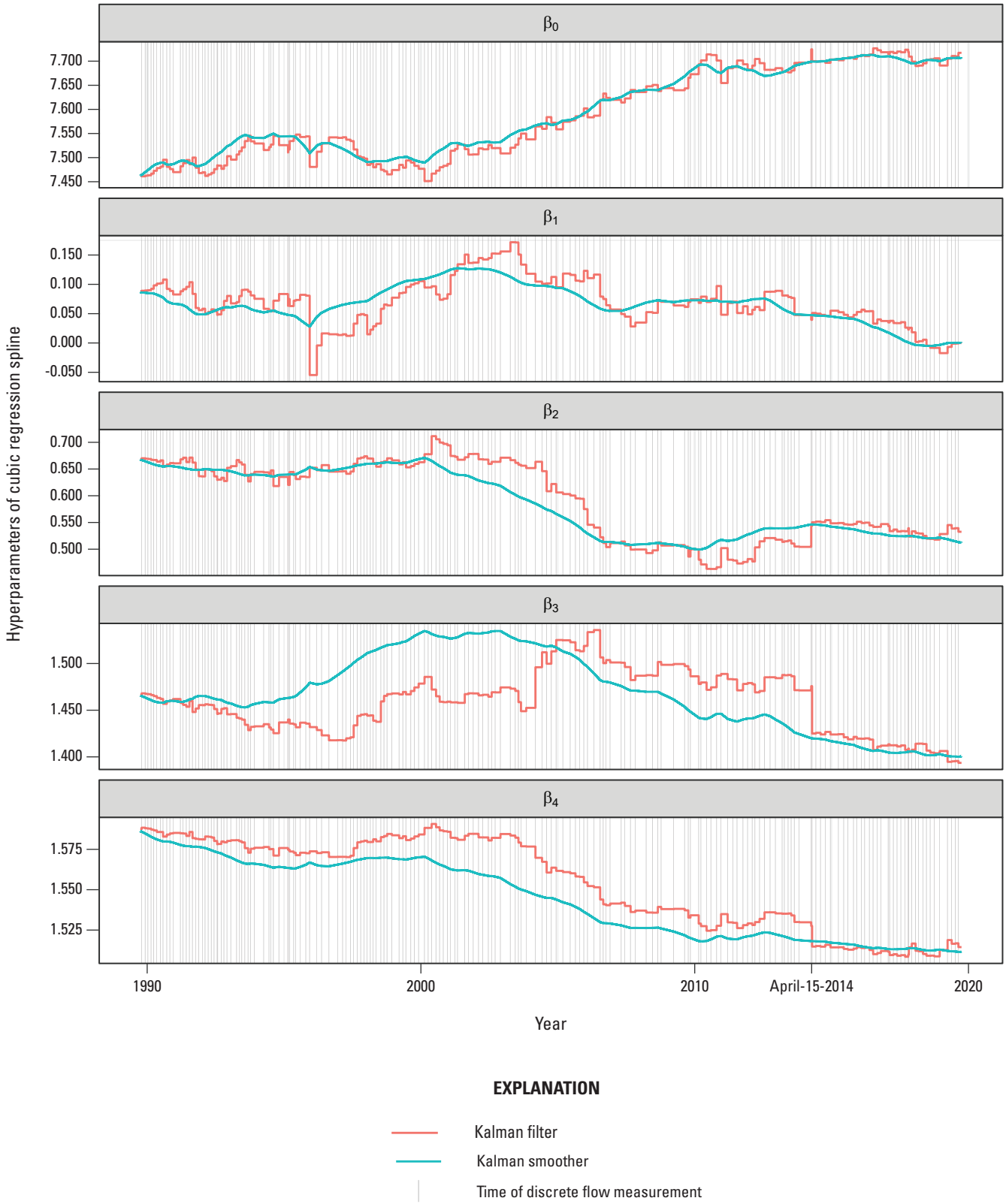

Figure 11. Hyperparameters of cubic regression spline developed in state-space model 6 for U.S. Geological Survey streamgage 04122500 Pere Marquette River at Scottville, Michigan.

for a localized effect of discrete measurements on model hyperparameters is provided by the measurement number 659 on April 15, 2014, which was the second highest discrete measurement during the period of record with measured discharge of 4,830 ft^3/s and a stage of 6.63 ft of gage height.

Specifically, on April 15, 2014, a substantial decrease (-0.05) was measured in the filtered estimate of parameter β_3, which corresponds to basis 3 with a knot at 6.42 ft of gage height. Lesser magnitude, at least with respect to the variability of the hyperparameters, but substantial changes were also measured in filtered estimates of parameters β_2 and β_4 with knot locations for corresponding basis of 4.75- and 8.10-ft of gage height, respectively. Only minor relative changes were measured in parameters β_0 and β_1. Thus, it appears that the closer the gage height is to a knot location of the basis, the more the corresponding hyperparameter may be affected.

The negative support for localized effect is based on the time series plot of β_4 (fig. 11). The filtered estimate, which is propagating forward through time, shows a substantial decrease in response to measurement 659 on April 15, 2014. The smoothed estimate, which is propagating backward through time, however, already reflects the information in measurement 659 and merely continues a steady drift upward using, in part, the filtered estimates. Although the smoothed estimate will have a smaller variance than the filtered estimate, it is not clear which estimate more closely reflects conditions in the field. Specifically, if the high discharge conditions on April 15, 2014 changed the hydraulic conditions, the filtered estimate may be preferred. Hydrographic analysis of flow conditions in the local streamgage network would be needed to determine the timing of shifts more precisely. In this report, however, the timing of changes in hyperparameters are based strictly on the timing of discrete measurements.

Stage-discharge Rating Adaptations with Discrete Measurements

Figure 12 shows biennial adaptations of the stage-discharge relations to discrete measurements from water year 1990 to 2018. Adaptations of the rating (in blue) are referenced to left bounding rating 18 and right bounding rating 21, both in grey. Discrete measurements in the corresponding water year are shown as points color coded by discharge measurement quality.

In 1990, the adaptive rating is consistent with rating 18. With increasing time, the adaptive rating shifts to the right in response to changes in regression spline hyperparameters determined by discrete measurements until it is generally consistent with rating 21. As the adaptive rating shown is based on the Kalman smoothed hyperparameters, the shift by discrete measurement number 659 at a stage of 6.63 ft and discharge of 4,830 ft^3/s may be reflected in changes in shape of the adaptive rating in some of the preceding years. In cases where this full backward propagation through time is not thought to be appropriate, the span of the Kalman smoothed might be shortened or the Kalman filtered hyperparameters may be substituted.

Discharge Magnitudes and Uncertainties of the Kalman Smoothed Discharges

Figure 13 shows daily discharge information and discrete measurements for selected years at the Pere Marquette streamgage from 1990 to 2018. Discharge information includes published daily mean discharge and the Kalman smoothed discharge estimate with a 95-percent confidence interval. Shaded regions generally indicate ice-affected discharge, which is shown as the region between the published daily discharge and the Kalman smoothed discharge estimate.

The Kalman smoothed estimates of daily mean discharge and the associated confidence interval were generally based on the mean of unit stage values for the day. On days of discrete measurements, however, the discrete measurement of stage was substituted for the daily mean stage, and the discrete measurement of discharge was substituted for the daily mean discharge, as discussed under the development of the y time series in section "Measurement Time Series of Discrete Discharges." In contrast, published daily mean discharges were based on the average of unit discharges computed from unit stage values, except during ice-affected periods when unit stage may be an unreliable indicator of discharge. The Kalman smoothed estimates of ice-affected discharge—which are based on stage data and did not include ice-affected discrete measurements or regression estimates of discharge—are currently unusable. These factors explain some of the differences among the lines in figure 13.

For the 30-year period of analysis, about 99.2 percent of estimated discharge happens during the 106-day period from December 1 to March 15. During this cold-weather period, about 42.1 percent of the daily mean discharges are estimated. Much of the estimated discharge during cold-weather periods results from missing stage data or variable ice-backwater conditions that make stage a less reliable indicator of discharge. Instead, published daily mean discharge is commonly estimated by hydrographic comparison techniques (Rantz, 1982b), which has uncertainties that are difficult to characterize.

Comparison of Rated and Smoothed Discharges with Published Daily Means

Daily mean discharges published by the USGS are generally classified as computed or estimated. Computed discharges generally refer to unit flows based on a stage-discharge rating and unit stage values. Computed daily mean discharges aggregate unit flows. The accuracy of computed flows is thought to be quite high, but uncertainties are difficult to quantify because of the continual application of subjective rating

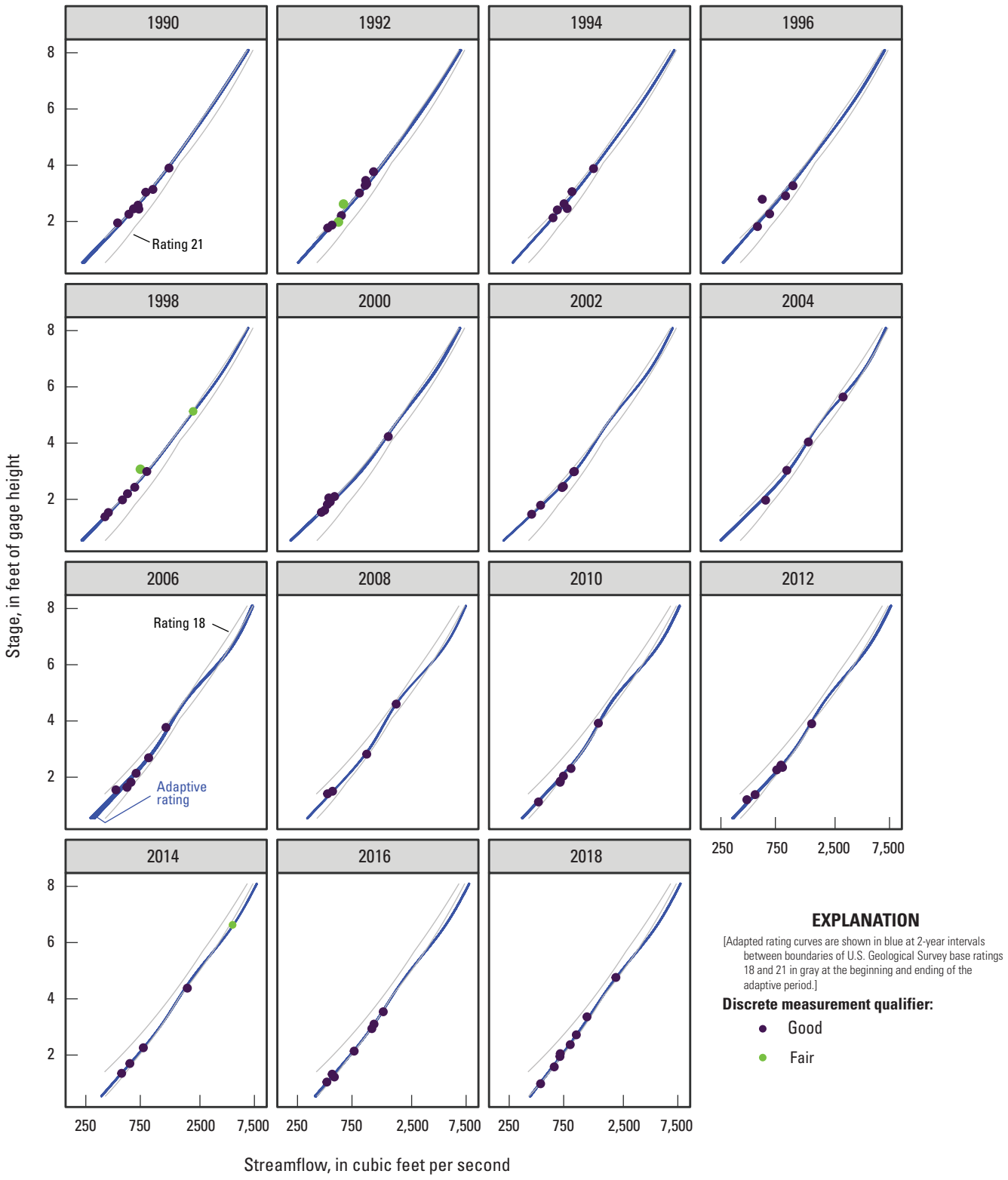

Figure 12. Adapted rating computed using Kalman smoothing parameters with discrete measurements from 1990 to 2018 for U.S. Geological Survey streamgage 04122500 Pere Marquette River at Scottville, Michigan.

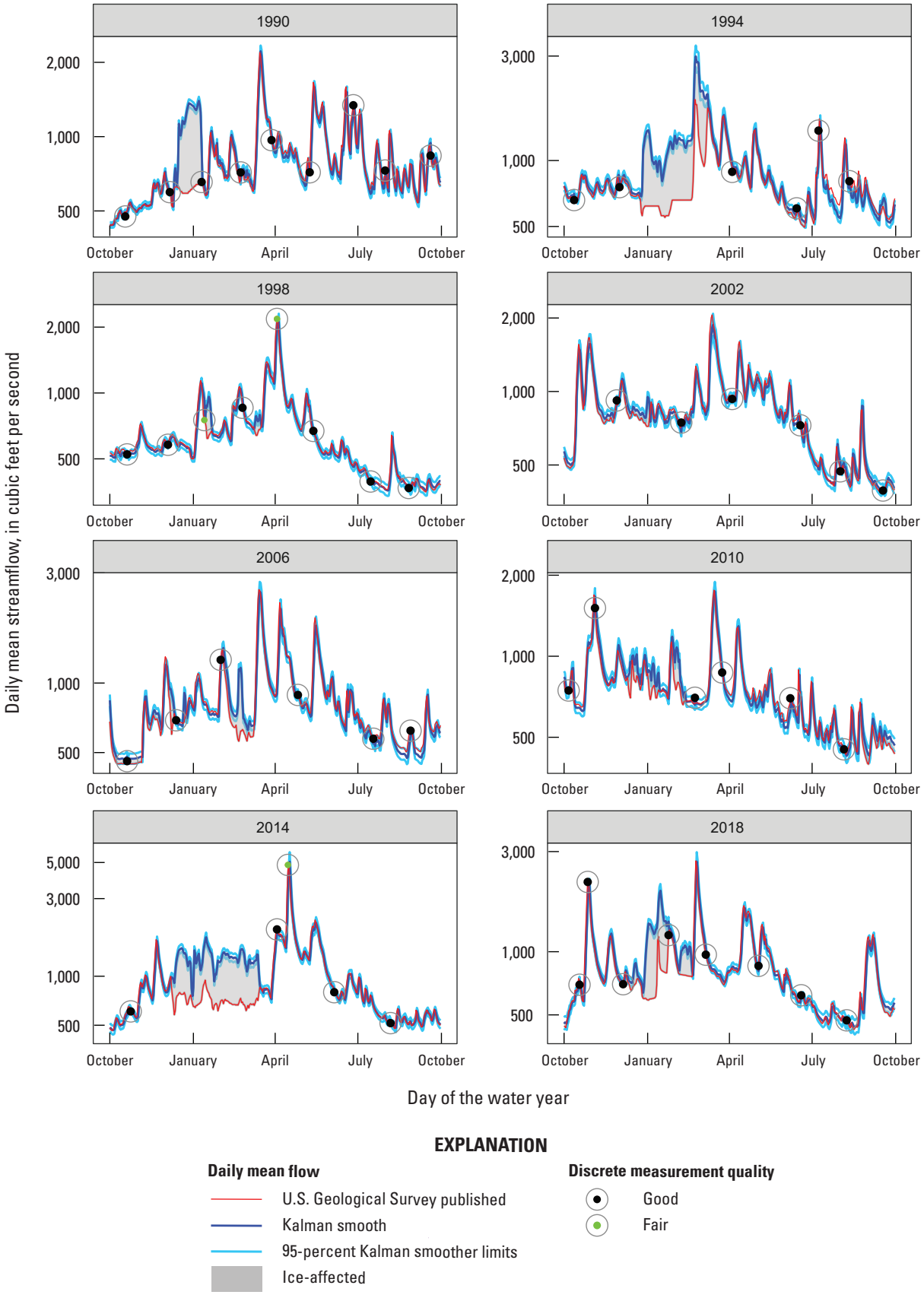

Figure 13. Measures of daily mean discharge magnitudes and uncertainties for selected water years at U.S. Geological Survey streamgage 04122500 Pere Marquette River at Scottville, Michigan.

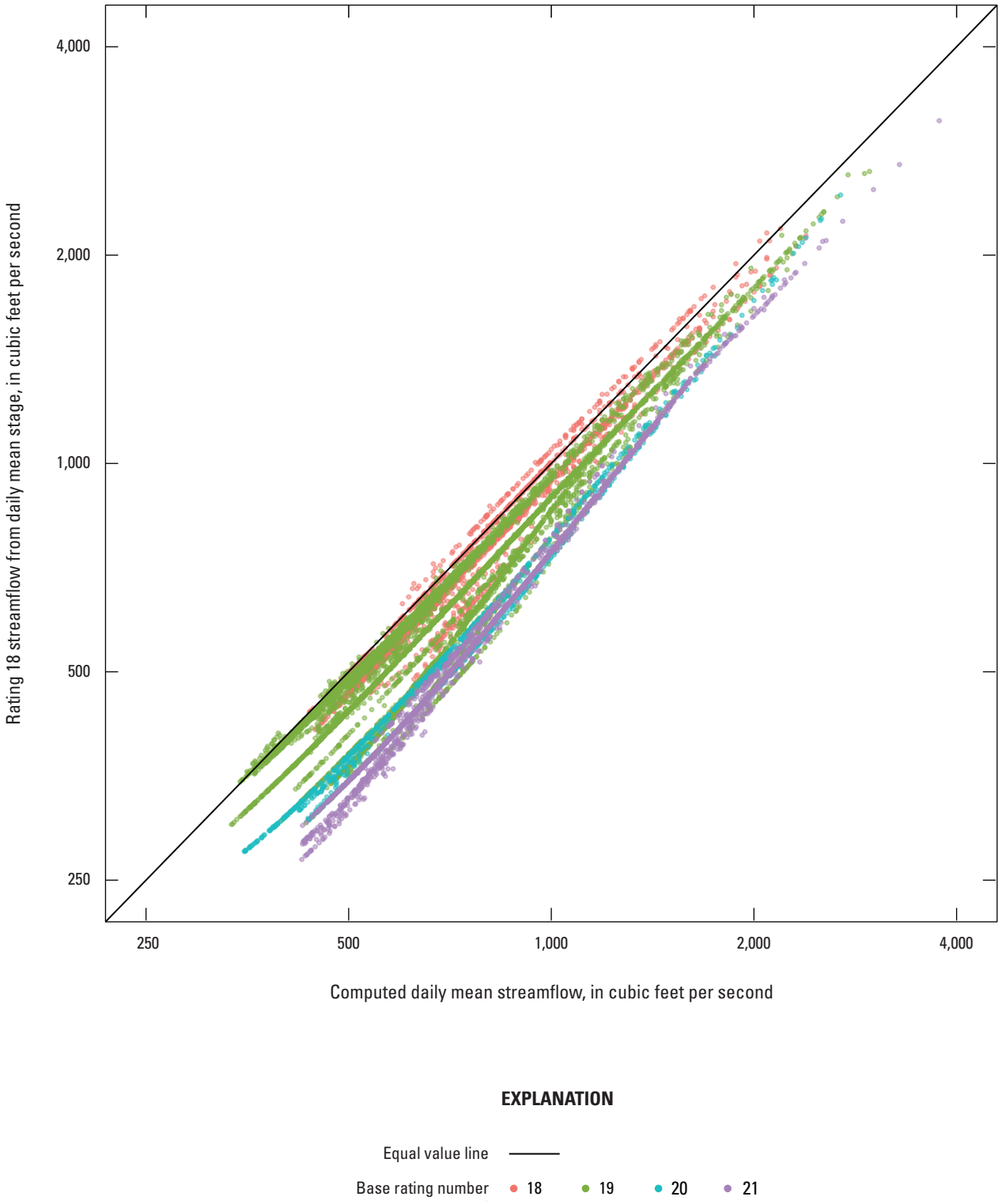

Figure 14. Relation between discharges computed with rating 18 and published daily mean discharges for water years 1990 through 2019 at U.S. Geological Survey streamgage 04122500 Pere Marquette River at Scottville, Michigan.

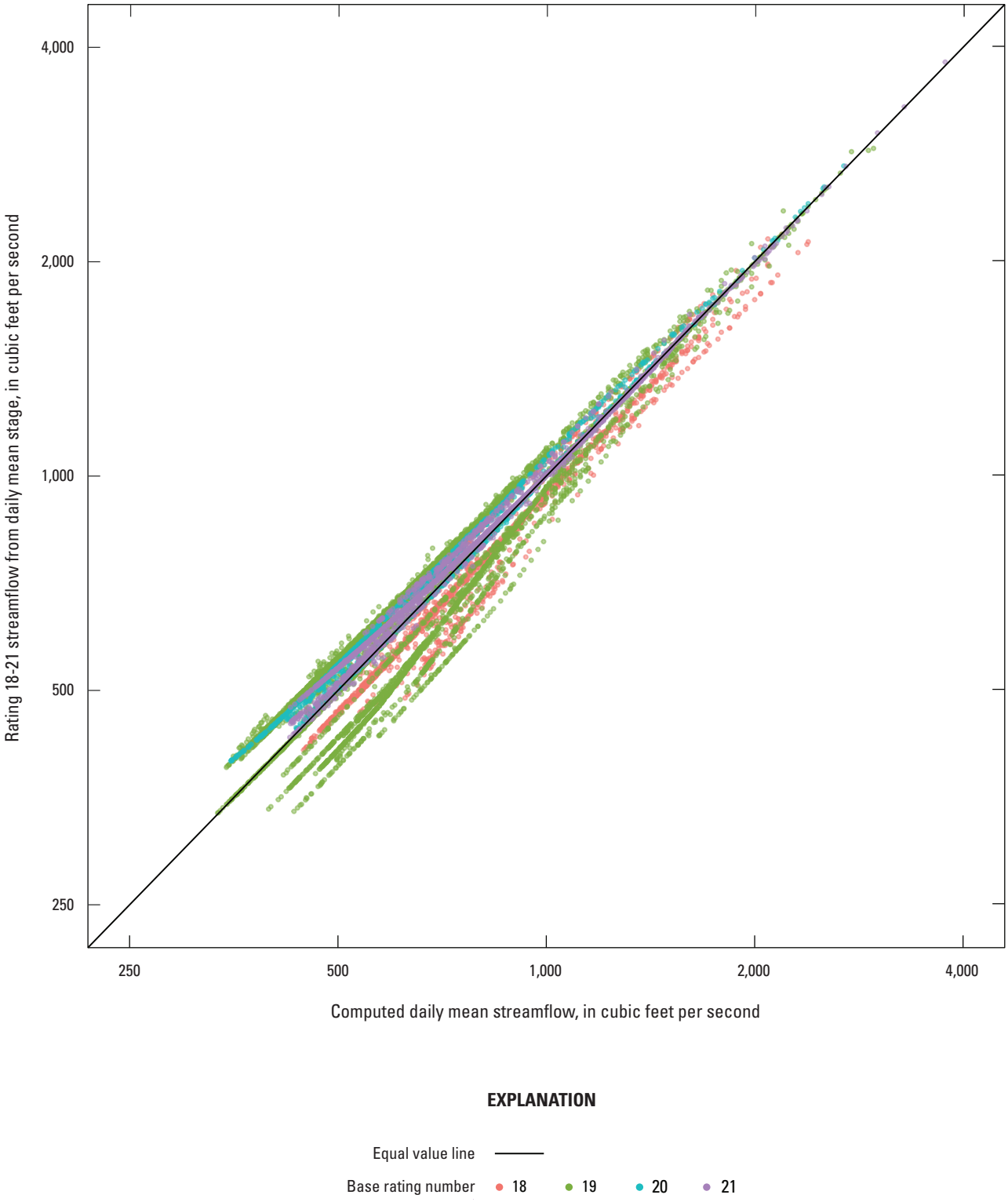

Figure 15. Relation between discharges computed with base ratings 18–21 and published daily mean discharges for water years 1990 through 2019 for U.S. Geological Survey streamgage 04122500 Pere Marquette River at Scottville, Michigan.

adjustments. In contrast, estimated daily mean discharges are usually based on the relation between flows at the target streamgage with flows in nearby streamgages.

Figure 14 shows daily mean discharges computed with daily mean stage values using base rating 18 for water years 1990–2019. The figure shows that base rating 18 initially tracked the published discharges closely but that the accuracy of the flows computed with this simplification degraded with time, with greater divergence apparent at lower flows. The accuracy of this flow information is comparable to the flows that would be computed if discrete measurements and rating adjustments were terminated after rating 18 was developed.

Figure 15 shows a substantial reduction in bias and variance between published discharges and discharges computed simply by application of base ratings 18–21 when they were applicable as a base rating. The transitions to different base ratings might be thought of as accounting for major cumulative shifts in the previous stage-discharge rating. The effect of within base-rating-period shifts and adjustments are not accounted for in discharges computed from the base ratings, but the shifts and adjustments were computed, requiring time and skillful application of the hydrographer's tools for describing shifts.

Figure 16 shows the relation between published daily mean discharges and smoothed discharges based on daily mean stages. There are no other base rating periods that are relevant to the analysis, but the daily values are color coded for consistency with figures 14 and 15. Instead of continual analysis of base ratings and shifts, the hyperparameters of cubic regression parameters describing the stage-discharge rating varied in response to discrete measurements of stage and discharge, with the uncertainty of discharge characterized by R. Fluctuations in hyperparameters and the shape of the rating were modulated by Q, which controls the variance of hyperparameters and the stability of the stage-discharge relation. The mathematics of the filtered (real time) and smoothed (final) values can be used to compute the uncertainty of the time series of unit discharge values after Q is rescaled for unit value computations. The correlation between the logs of computed daily mean discharges and Kalman smoothed discharges 0.9791.

Differences between natural logs can be closely approximated by differences in percent given that the differences are small in magnitude but are somewhat asymmetrical; for example, differences of 0, ±5-, and ±10-percent correspond to interval bounds for natural logs of [0], [−0.049, 0.051], and [−0.05, 0.15], respectively. To simplify interpretation, the interval bounds in natural log units are expressed as if they were percentages in the following discussion.

Figure 17 shows the distribution of differences between the natural logs of smoothed discharges and computed daily mean discharges. The distribution is approximately symmetrical with a mean of zero indicating little bias. About 85 percent of these differences are within the high-density interval from [−9.92, 9.47] percent, and about 50 percent of the differences fall within the high-density interval from [−2.75, 5.25] percent. The published daily mean discharges and the Kalman smoothed discharges contain uncertainties that may be associated with suboptimal shift magnitudes or timings.

On days of discrete measurements, the 85-percent high-density interval about the differences between filtered and included discrete flow measurements was [−7.60, 9.18] percent, and the 50-percent interval was [−6.07, 1.45] percent. Also, on days of discrete measurements, the 85-percent high-density interval about the differences between smoothed and measured flow was [−6.35, 5.58] percent, and the 50-percent interval was [−2.82, 2.21] percent. Some of this variability may be associated with a discrepancy between the published daily mean discharge and the discrete measurement of discharge on that day.

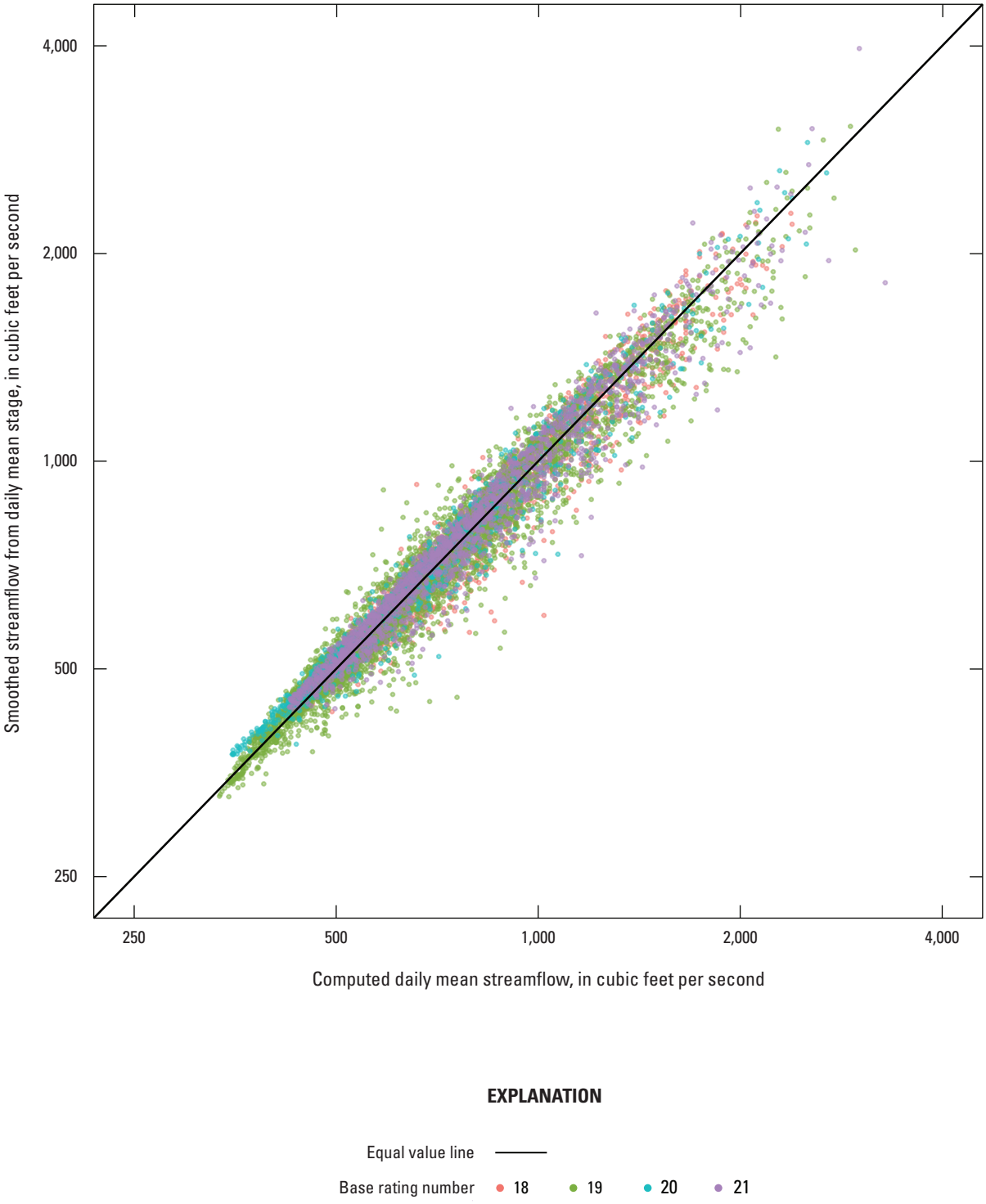

Figure 16. Relation between Kalman smoothed discharge estimates and published computed daily mean discharges for water years 1990 through 2019 for U.S. Geological Survey streamgage 04122500 Pere Marquette River at Scottville, Michigan.

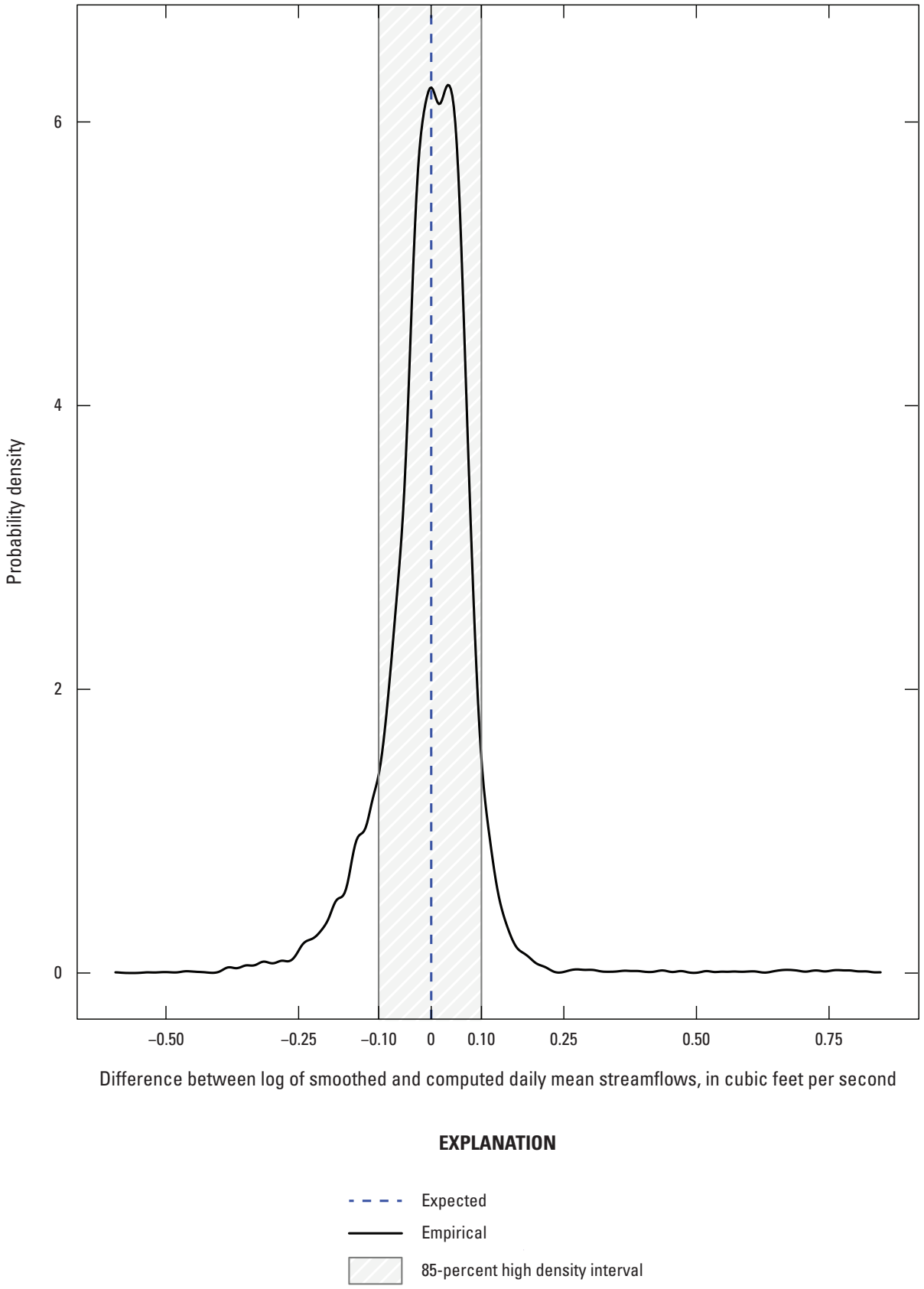

Figure 17. Distribution of differences between smoothed and computed daily mean discharges for water years 1990 through 2019 at U.S. Geological Survey streamgage 04122500 Pere Marquette River at Scottville, Michigan.

Limitations

The proposed state-space Kalman estimation approach provides a basis for computing filtered and smoothed estimates of hyperparameters of a CRSs that adapt the stage-discharge relation for discrepancies indicated by each open-water discrete discharge measurement. A limitation of this approach is that discrete measurements, which are typically 6 to 8 weeks apart, do not generally correspond to the actual timing of changes in the stage-discharge relation. Hydrographers have commonly used hydrograph comparison techniques (Rantz, 1982b) to improve their understanding of the timing. An adaptation of the form of the state-space model developed in this report and inclusion of network flow information is needed to compute ice-affected discharges.

Using the proposed state-space Kalman estimation approach, the temporal resolution for detecting the timing of changes in the stage-discharge rating may be improved by estimating discharges on days without discrete measurements using discharge records from other streamgages in the network. Estimates may be improved by first adjusting for travel-time lags between discharges at the predictor streamgages with discharges at the target streamgage. For the target streamgage, periods of discrete measurements may be identified for comparison with the lag-adjusted discharges at predictor streamgages through regression analysis. Regression estimates of discharge at the target streamgage may be encoded in the y time series for periods without discrete measurements. Similarly, corresponding prediction variances could be used to populate values of the measurement error variance matrix R. Once the Q matrix is rescaled from daily values to the preferred unit time step and the elements of y and R augmented with values based on network discharges, the unit discharges and their uncertainties could be recomputed using the Kalman estimator without re-estimating other parameters in the state-space model; for example, strategic placement of regression estimates of discharge at times near the onset or dissipation of ice-effects with alternative parameterizations of the process error covariance matrices Q_{open} and Q_{ice} for open-water and ice-affected conditions may facilitate the rapid adaptation of the open-water to ice-affected conditions even when discrete measurements are relatively sparse.

Summary and Conclusions

A computer-aided approach is developed for adapting stage-discharge relations to changing hydraulic conditions indicated by discrete measurement data. In addition, the approach provides a basis for computing the magnitudes and uncertainties of unit and daily streamflow data. Methods comprising the approach include: (1) development of a cubic regression spline (CRS) model of an initial stage-discharge relation; (2) specification of a state-space model in which the state vector $\boldsymbol{x}$ is initialized with the spline parameters from the CRS, the observation time series y contains logarithms of measured flow values at times of discrete measurements, and NA indicators otherwise; (3) estimation of state-space model parameters Q and R for the process-error covariance matrix and the measurement-error variance; and (4) application of Kalman filtering and smoothing to compute the magnitudes and uncertainties of unit or daily streamflow data for real-time and offline use. A case study using streamflow data from USGS streamgage 04122500 Pere Marquette River near Scottsville, Michigan, is used to illustrate the approach using the mixed generalized additive model (GAM) computation vehicle (mgcv) package for CRS development and the Multivariate Auto-Regressive State Space (MARSS) package for state-space modeling in the R programming and computing environment.

The approach is initiated by developing a CRS of stage-discharge relations at the beginning of the period of analysis. CRSs are estimated directly from existing rating tables or from sets of discrete stage-discharge measurements. Estimation of the parameters of a CRS from an existing rating may provide flows that smoothly transition from a rating developed with manual adaptations to one developed with computer-aided adaptations. Estimation of CRS parameters from a set of discrete stage-discharge measurements may be preferred for streamgages without an existing rating.

Parameters of the CRS form the initial state vector $\boldsymbol{x}_0$ in the state-space model, which is composed of a state equation and a measurement equation. The two equations are solved alternately at each time step in the analysis. Within the state equation, a temporal update is computed by premultiplying the state vector by the transition matrix, B. This temporal update is associated with an increase in the variance of elements in the state vector, which is quantified as the state-error covariance matrix P. The increment in variance is determined by the magnitudes of elements in the process-error covariance matrix Q.

Within the measurement equation, the temporally updated state vector is premultiplied by the design array $\boldsymbol{Z}$, which contains the basis vector for the corresponding stage. The matrix multiplication results in a scalar estimate of flow that can be compared with any discrete measurement of flow data available at that time step. These differences were minimized to estimate parameters in the Q and R matrices.

Stage and discharge data from the Pere Marquette streamgage were used as a case study. Changes in the stage-discharge relation were tracked across the 30-year period of analysis from October 1, 1989, to September 30, 2019, when ratings 18–21 were in effect. A CRS was developed by use of stage and discharge values defining rating table 18. Five knots and a link function for the gamma distribution were specified for the CRS. The five-knot specification resulted in a five-parameter CRS and the link function effectively resulted in a natural logarithmic (log) transformation of streamflow values. This CRS explained essentially all the variability in the data forming rating table 18.

Parameters of this CRS formed the initial state vector x_0 in a state-space model. Parameters of the state-space model in the Q and R matrices were estimated at daily time steps using available ice-free discrete measurement data and basis vectors computed from daily mean stage values and knot locations for the 30-year period of analysis. Six alternative state-space models with different forms for the Q and R matrices were estimated. The model with the minimum Akaike information criterion statistic was selected to illustrate the estimation results. This model contained one parameter for a 5×5 diagonal Q matrix having equal variances. The variances for the 1×1 R matrix series were based on the hydrographer's field estimate of discrete measurement quality and their associated measurement variances. Although the estimate of the Q matrix was based on daily time steps, the variances can be rescaled for unit time step applications.

Adaptations of the spline describing the stage-discharge rating happens at each discrete measurement. In filtering, changes in the state vector (the hyperparameters of the spline) is a step function at the time of discrete measurements. In smoothing, these changes are more continuous. Changes in the hyperparameters gradually change the shape and location of the spline curve with time.

At the Pere Marquette streamgage, the stage required to pass most discharges generally decreased during the 30-year period of analysis. Thus, higher numbered ratings are always to the right of lower numbered ratings. The transition of the computed-adapted spline from rating 18 to 21 is shown at 2-year intervals. This sequence begins at rating 18 and steadily progresses through time spanning the interval between ratings 18 and 21 while generally being bounded by these ratings. Elements of the hyperparameter vector appear to be affected locally based on the proximity of their knot locations to the discrete stage measurement. These characteristics support the ability of the proposed approach to aid the adaptation of the stage-discharge rating to changes in rating conditions based on discrete discharge measurements.

The filtered and smoothed daily mean flows were consistent with the computed daily mean flows. A comparison of logarithms of publish daily mean discharges based on values qualified as computed and Kalman smoothed discharges indicates a coefficient of determination (r^2) value of 0.9587. The 85-percent high-density interval between differences of logarithms of published discharges and smoothed discharges had boundaries of approximately [−9.92, 9.47] percent. A refinement of the methodology would include a mechanism to improve the understanding of the timing of shifts at a resolution finer than the frequency of discrete measurements currently enable.

References Cited

Aquatic Informatics, 2022, Aquarius WebPortal: Non-Administrative User Guide (ver. 2022.1): Vancouver, British Columbia, 64 p., accessed June 17, 2022 at https://waterdata.ibwc.gov/Content/Manuals/en/UserGuide.pdf.

De Cicco, L.A., Lorenz, D., Hirsch, R.M., and Watkins, W., 2018, dataRetrieval—R packages for discovering and retrieving water data available from Federal hydrologic web services (ver. 2.7.4): U.S. Geological Survey code web page, accessed June 17, 2022, at https://doi.org/10.5066/P9X4L3GE.

Delignette-Muller, M.L., and Dutang, C., 2015, fitdistrplus—An R package for fitting distributions: Journal of Statistical Software, v. 64, no. 4, p. 1–34, accessed June 17, 2022, at https://www.jstatsoft.org/v64/i04/.

Holmes, E.E., Ward, E.J., Scheuerell, M.D., and Wills, K., 2020a, MARSS—Multivariate Autoregressive State-Space Modeling package: R Project web page, accessed June 17, 2022, at https://cran.r-project.org/web/packages/MARSS/index.html.

Holmes, E.E., Ward, E.J., and Scheuerell, M.D., 2020b, Analysis of multivariate time-series using the MARSS package (ver. 3.11.3): R Project web page, accessed June 17, 2022, at https://cran.r-project.org/web/packages/MARSS/vignettes/UserGuide.pdf.

Holtschlag, D.J., and Miller, R.L., 1998, Streambed stability and scour potential at selected bridge sites in Michigan: U.S. Geological Survey Water-Resources Investigation Report 98–4024, 84 p., accessed June 17, 2022, at https://doi.org/10.3133/wri984024.

Maechler, M., 2021, Statistical data analysis in seminar in statistics: Zurich, Switzerland, Swiss Federal Institute of Technology, accessed May 18, 2021, at https://stat.ethz.ch/R-manual/R-devel/library/mgcv/html/vcov.gam.html.

Makowski, D., Ben-Shachar, M.S., and Lüdecke, D., 2019, bayestestR—Describing effects and their uncertainty, existence and significance within the Bayesian Framework: Journal of Open Source Software, v. 4, no. 40. [Also available at https://doi.org/10.21105/joss.01541.]

Rantz, S.E., 1982a, Measurement and computation of streamflow volume 1—Measurement of stage and discharge: U.S. Geological Survey Water-Supply Paper 2175, 313 p., accessed June 17, 2022, at https://doi.org/10.3133/wsp2175.

Rantz, S.E., 1982b, Measurement and computation of streamflow volume 2—Computation of discharge: U.S. Geological Survey Water-Supply Paper 2175, 373 p., accessed June 17, 2022, at https://doi.org/10.3133/wsp2175.

R Core Team, 2021, R—A language and environment for statistical computing: R project web page, accessed May 7, 2021, at https://www.R-project.org/.

Simon, D., 2006, Optimal state estimation—Kalman, h-∞, and nonlinear approaches: Hoboken, N.J., John Wiley & Sons, Ltd., 526 p.

Shumway, R.H., and Stoffer, D.S., 2016, Time Series Analysis and Its Applications with R Examples (4th ed.): Springer Texts in Statistics, 558 p., accessed June 17, 2017 at http://www.stat.pitt.edu/stoffer/tsa4.

U.S. Environmental Protection Agency, 2000, National water quality inventory—1998 report: U.S. Environmental Protection Agency Report EPA–841–F–00–006, 45 p. [Also available at https://water.epa.gov/lawsregs/guidance/cwa/305b/98report_index.cfm.]

U.S. Geological Survey, 2011, Discharge measurement quality code: U.S. Geological Survey National Water Information System database, help system web page, accessed June 2021 at https://doi.org/10.5066/F7P55KJN. [Help system page directly accessible at https://help.waterdata.usgs.gov/codes-and-parameters/discharge-measurement-quality-code.]

U.S. Geological Survey, 2022, USGS 04122500 Pere Marquette River at Scottville, MI, *in* USGS water data for the Nation: U.S. Geological Survey National Water Information System database, accessed January 2022, at https://doi.org/10.5066/F7P55KJN. [Site information directly accessible at https://waterdata.usgs.gov/nwis/inventory/?site_no=04122500&agency_cd=USGS&.]

Wood, S.N., 2006, Generalized additive models—An introduction with R (1st ed.): Boca Raton, Fla., CRC Press, 392 p.

Wood, S.N., 2017, Generalized additive models—An introduction with R (2d ed.): Boca Raton, Fla., CRC Press, 496 p.

Wood, S.N., 2021, mgcv—Mixed GAM computation vehicle with automatic smoothness estimation (ver. 1.8-36): R Project web page, accessed June 4, 2021, at https://cran.r-project.org/web/packages/mgcv/index.html.

For more information about this publication, contact:
Director, USGS Upper Midwest Water Science Center
1 Gifford Pinchot Drive
Madison, WI 53726
608–828–9901
For additional information, visit: https://www.usgs.gov/centers/upper-midwest-water-science-center
Publishing support provided by the
Indianapolis Publishing Service Center

ISSN 2328-0328 (online)
https://doi.org/10.3133/sir20225083